NASA CR 54814
AGC 8800-49

FABRICATION OF LIGHTWEIGHT TURBINE
COMPONENTS USING ELECTRON - BEAM WELDING
FOR THE ATTACHMENT OF SHEET METAL BLADES
TO DISCS AND SHROUDS

By

R. Beer

Prepared for

National Aeronautics and Space Administration

Contract NAS 3-2555

AEROJET
GENERAL TIRE
GENERAL

AEROJET-GENERAL CORPORATION

SACRAMENTO. CALIFORNIA

TECHNOLOGY REPORT

FABRICATION OF LIGHTWEIGHT TURBINE COMPONENTS

USING ELECTRON-BEAM WELDING

FOR THE ATTACHMENT OF SHEET METAL BLADES TO DISCS AND SHROUDS

Prepared for

NATIONAL AERONAUTICS AND SPACE ADMINISTRATION

14 October 1966

CONTRACT NAS 3-2555

Prepared by: Technical Management:

AEROJET-GENERAL CORPORATION   NASA LEWIS RESEARCH CENTER
LIQUID ROCKET OPERATIONS   CLEVELAND, OHIO
SACRAMENTO, CALIFORNIA

AUTHOR: R. Beer   TECHNICAL MANAGER: D. D. Scheer

APPROVED: W. E. Watters   APPROVED: W. A. Tomazic
           Manager   M-1 Project Manager
           M-1 Turbopump Project

ABSTRACT

The design selection and the fabrication techniques used to produce the turbine components for the oxidizer turbopump of the M-1 Engine are described. The nozzle, reversing vane, and rotor assemblies discussed were fabricated from Inconel 718. The electron-beam welding process was used to construct the sheet metal blades as well as to attach them to the discs or shrouds.

TABLE OF CONTENTS

List of Figures (cont.)

I.   SUMMARY

This report presents the design selection and the fabrication techniques used to produce the nozzle, rotor, and reversing vane assemblies for the M-1 oxidizer turbine. These assemblies are constructed from Inconel 718. In all cases, the hollow sheet metal blades are electron-beam welded to the disc and the shroud or both shrouds (as in the case of the stationary parts). The weld joints are supplemented by brazing for vibration dampening. After considerable effort, a joint configuration was developed that successfully solved the difficult task of attaching the hollow sheet metal blades to a rotor disc. The electron-beam weld process, which was selected to weld the joints, restricted vendor selection to those few having electron-beam welding equipment of sufficient power and chamber size. The components described in this report were fabricated by the Jet and Ordnance Division of Thompson-Ramo Wooldridge, Incorporated of Cleveland, Ohio.

II.   INTRODUCTION

The pumping system for the liquid propellant M-1 engine consists of two separate turbopumps, each having a direct-drive turbine. A gas generator supplies the combustion products of liquid oxygen and liquid hydrogen as drive gas to the turbines, which are arranged in series. Figure No. 1 shows a mock-up of the M-1 engine delineating the major components of the engine assembly.

The two-stage prototype turbine of the M-1 Oxidizer Turbopump (Figure No. 2) discussed in this report was preceded by a single-stage turbine design for the initial oxidizer turbopump development. A fir-tree attachment was provided in the single-stage turbine design to permit the attachment of shrouded rotor blades to the disc. To expedite fabrication, the first two rotors were manufactured with unshrouded blades. These were machined from a solid disc. The solidity of the preferred fir-tree design with shrouded replaceable blades was somewhat compromised to minimize the large blade overhang that would be required to achive the desired solidity.

Seeking to minimize weight while permitting the use of a shrouded design as well as eliminating any limitations upon solidity or other aerodynamic features of the Model II two-stage turbine, the Aerojet-General Corporation undertook a research to ascertain an economical method for fastening sheet metal blades to the rotor discs as well as to the rotor and stator shrouds.

Weight considerations dictated hollow rotor and stator blades, which were also desirable because they are not subjected to as severe thermal gradients as are the solid blades. During this study, the process of electron-beam welding was introduced for consideration. This process appeared to be most suitable for the design being considered. A design was finally selected wherein the blades are electron-beam butt welded in machined slots in the disc. These machine slots have the exact profile of the blade. However, this design utilized a new and unfamiliar material (Inconel 718) as well as a new and relatively undeveloped welding process (EB welding). As a result, a number of problems were encountered, but with appropriate development effort these were overcome.

OXIDIZER TURBOPUMP

TURBINE EXHAUST DUCT

GAS GENERATOR

FUEL TURBOPUMP

PROPELLANT UTILIZATION VALVE

CROSS-OVER DUCT
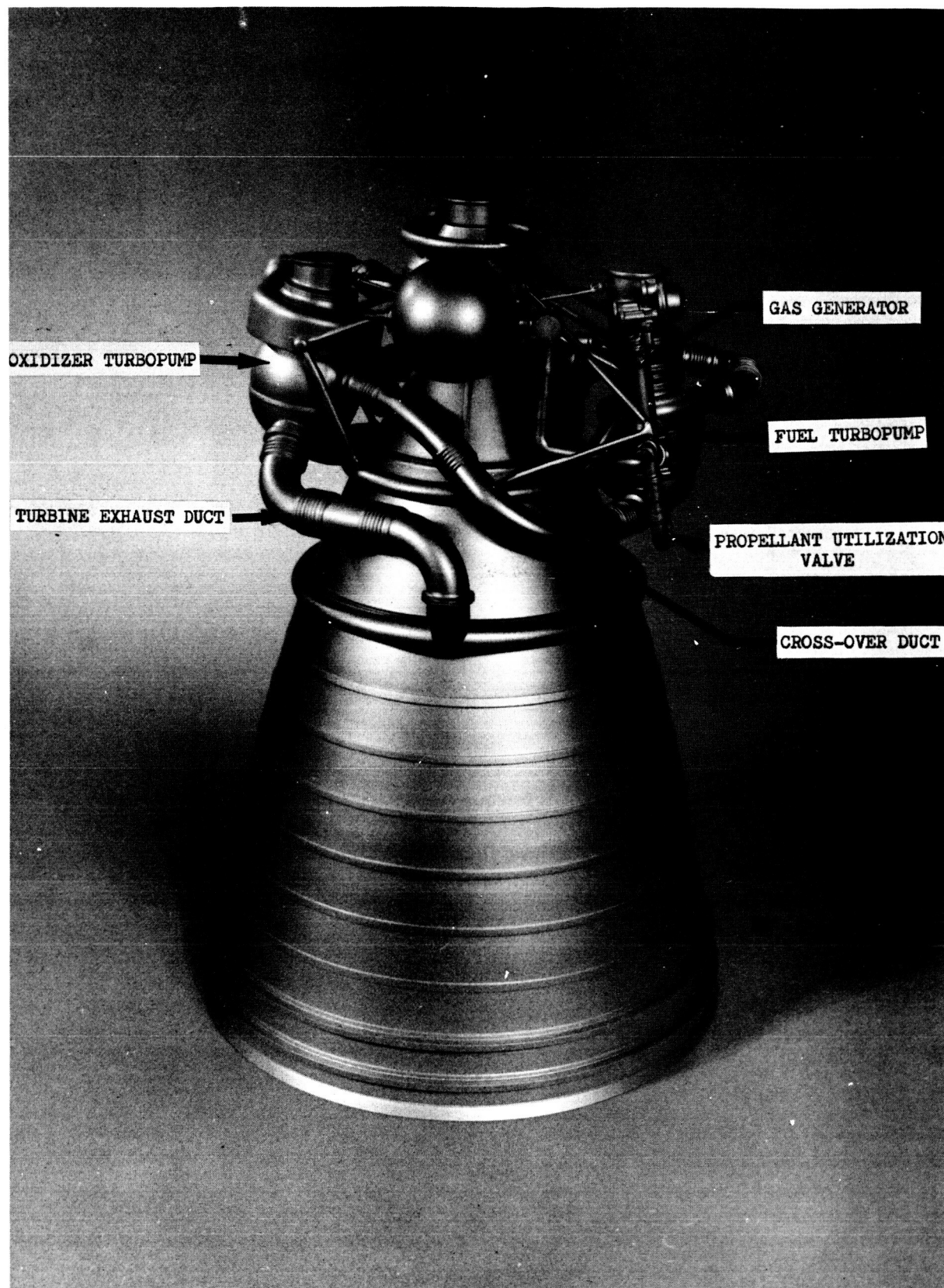
Figure 1

M-1 Engine Mockup
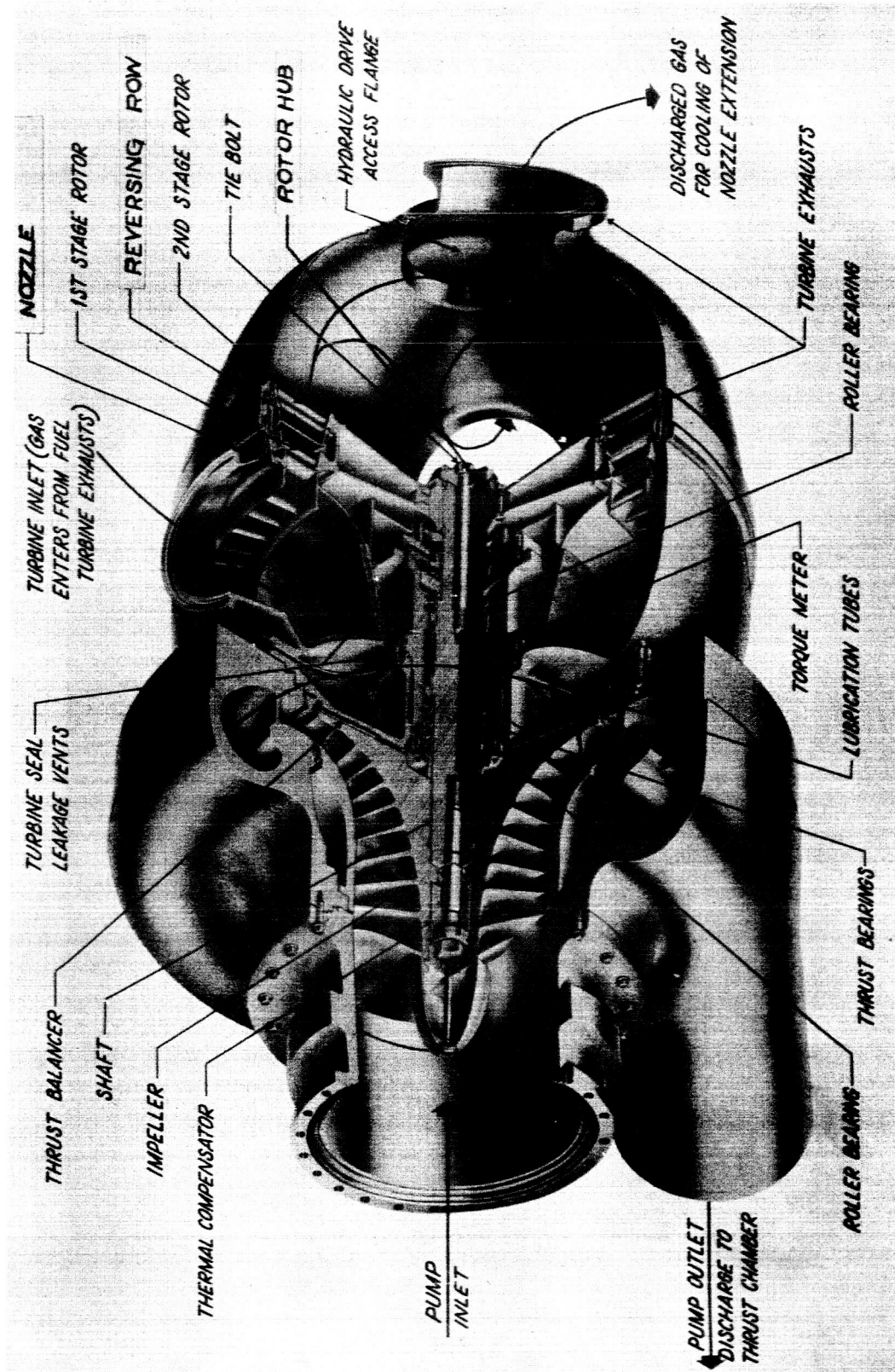
Figure 2

M-1 Oxidizer Turbopump Assembly

The nozzle and reversing vane assemblies were originally hollow blades that were gas tungsten arc welded (GTAW) to slots in the shrouds. These were also changed to electron-beam welded assemblies. This resulted from an experience where, in a similar design of another turbine, excessive weld shrinkage occurred during GTAW welding of the nozzles to the shroud, Figures No. 3, No. 4, and No. 5 show the completed nozzle assembly, the reversing vane assembly, and the completed rotor assembly, respectively.

The aerodynamic and mechanical design of the components discussed in this report have been described in previously published reports.[1][2]

The discussion in this report is largely concentrated upon those methods and procedures that are considered to be technological advances; conventional practices are not delineated.

III.   TECHNICAL DISCUSSION

A.   HARDWARE DESCRIPTION

Figure No. 2 shows the turbine components that are discussed in this report. These are the nozzle assembly (P/N 286513), the reversing vane assembly (P/N 286557), and the rotor assembly (P/N 286527). The rotor assembly is built up from the rotor subassembly stage 1 (P/N 286528), the rotor subassembly stage 2 (P/N 286533), and the rotor hub (P/N 1119263). The mean diameters of all of these assemblies is 33-in. which makes their size significant.

The two types of blades, the high reaction profile (Figure No. 6) designed for the nozzle and the low reaction, impulse, profile (Figure No. 7) designed for both rotors and the reversing vane assemblies are fabricated from 0.063-in. thick Inconel 718 sheet metal. In all instances, the blades are electron-beam (EB) welded into slots cut by means of the electrical discharge machining (EDM) process into stator shrouds as well as rotor discs and shrouds. Figure No. 8 shows a typical blade-to-disc and blade-to-shroud joint configurations.

1.   Rotor Assembly

This assembly is composed of the rotor hub, the rotor subassembly stage 1, and the rotor subassembly stage 2. The rotor hub is piloted on the shaft and the torque is transmitted from the hub to the shaft through a spline. A parallel face lug coupling acts as the interface between the rotor hub and the rotor disc subassemblies. This coupling transmits the torque and pilots the two sub-assemblies on the hub. Nine bolts are used to clamp the two conical discs together (see Figure No. 2).

---

[1] Beer, R., Aerodynamic Design and Estimated Performance of a Two-Stage Curtis Turbine for the Liquid Oxygen Turbopump of the M-1 Engine, NASA Report No. CR 54764, 19 November 1965

[2] Roesch, E., Mechanical Design of a Curtis Turbine for the Oxidizer Turbopump of the M-1 Engine, NASA Report No. CR 54815, 15 June 1966
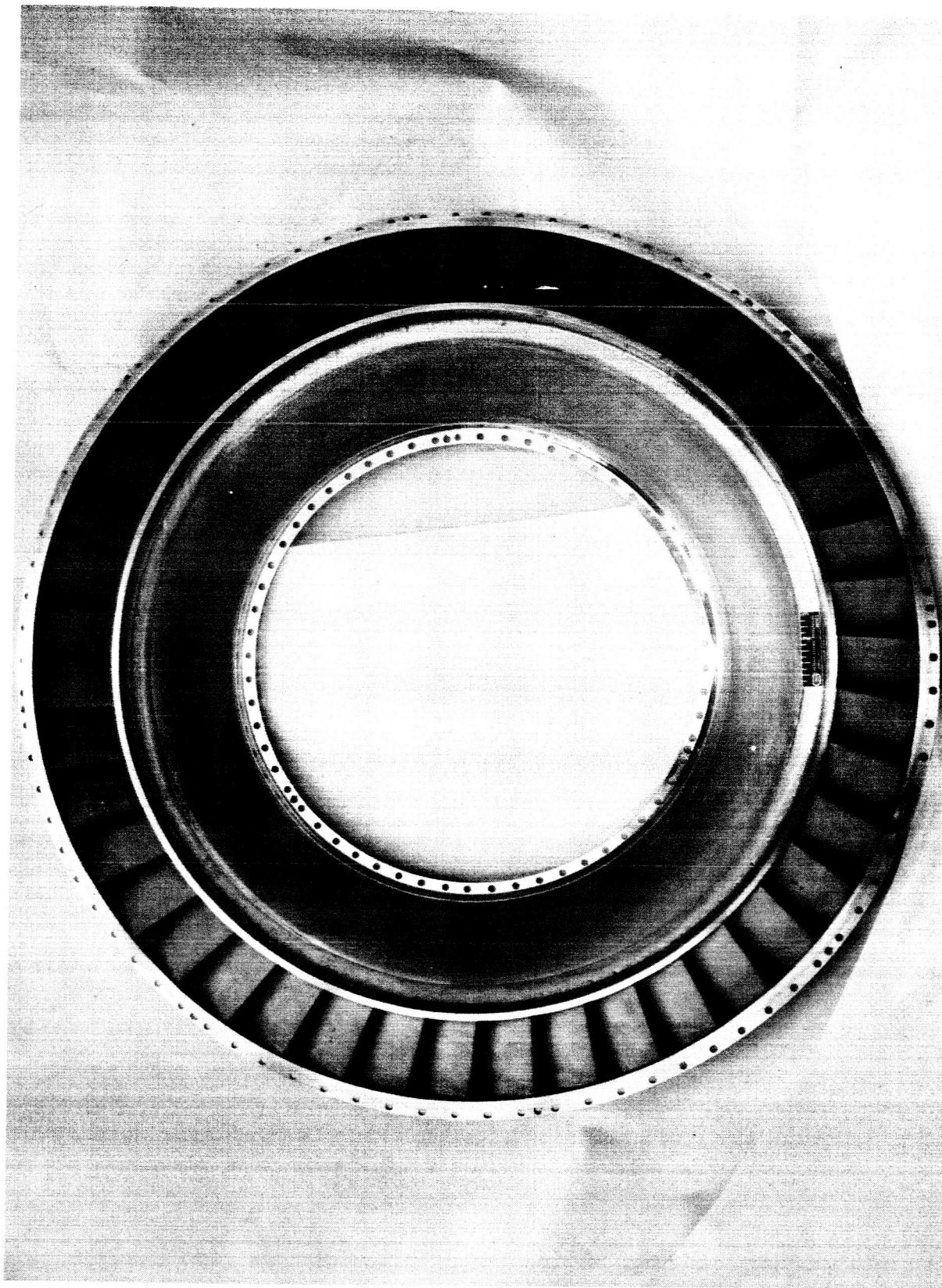
Figure 3

Nozzle Assembly

Page 5
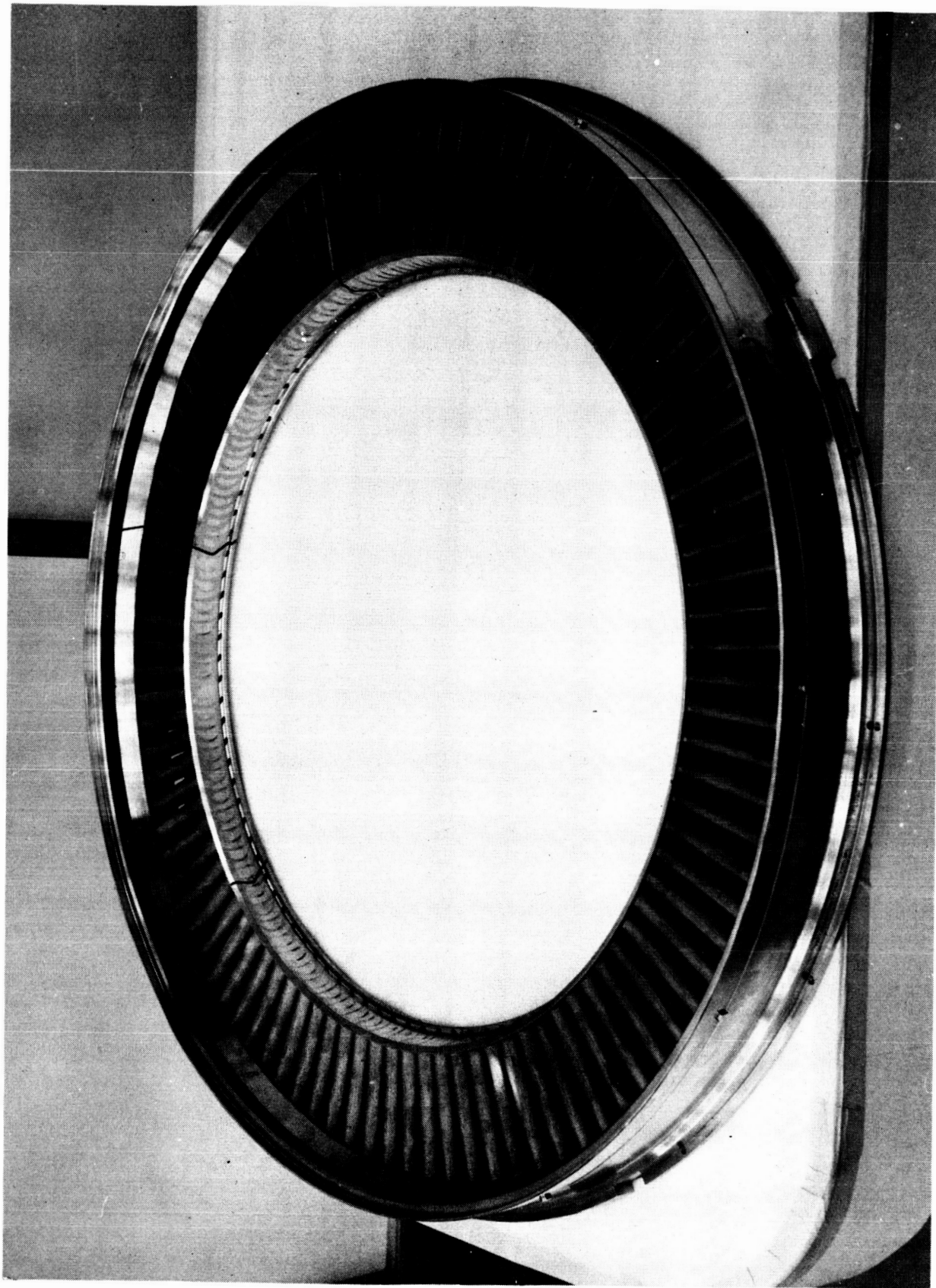
Figure 4

Reversing Row

Page 6

Figure 5

Rotor Assembly
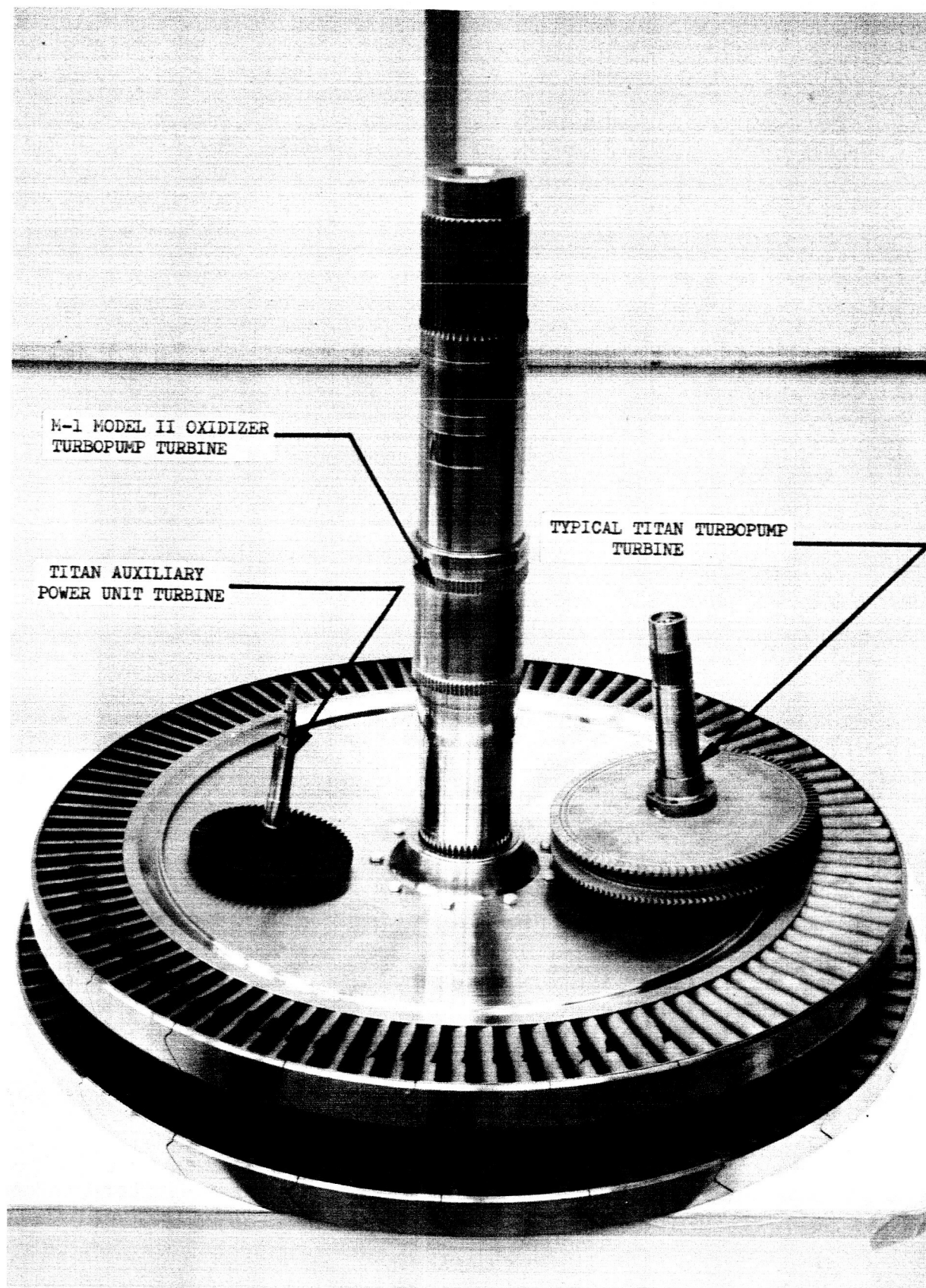
Figure 6

Nozzle Vane Profile

SMOOTH TRANSITION BETWEEN DEFINED POINTS
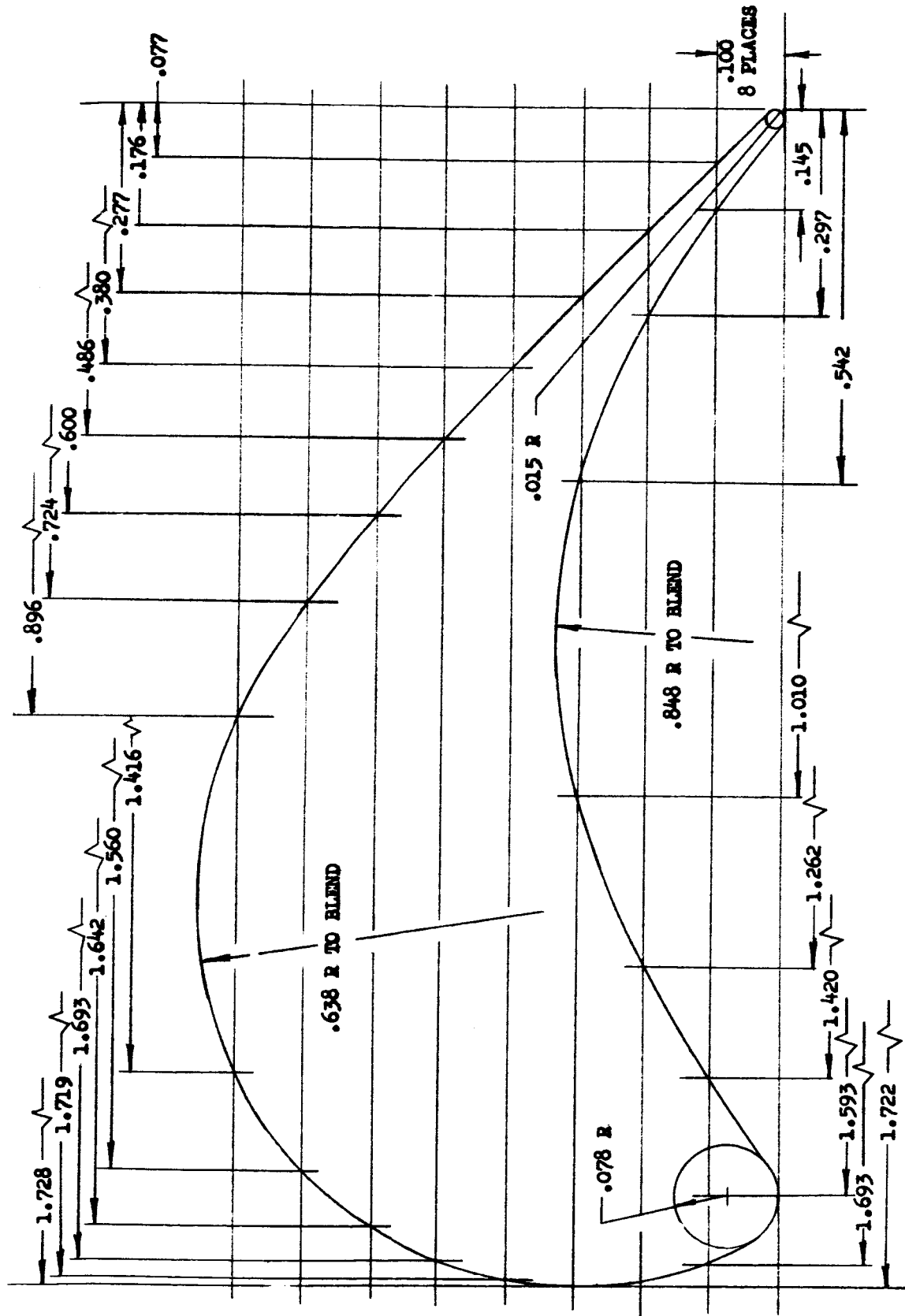
Figure 7

Rotor Blade and Reversing Vane Profile

PLUG

SHROUD

ELECTRON
BEAM WELD

BLADE

ELECTRON
BEAM WELD

INTEGRAL DISC
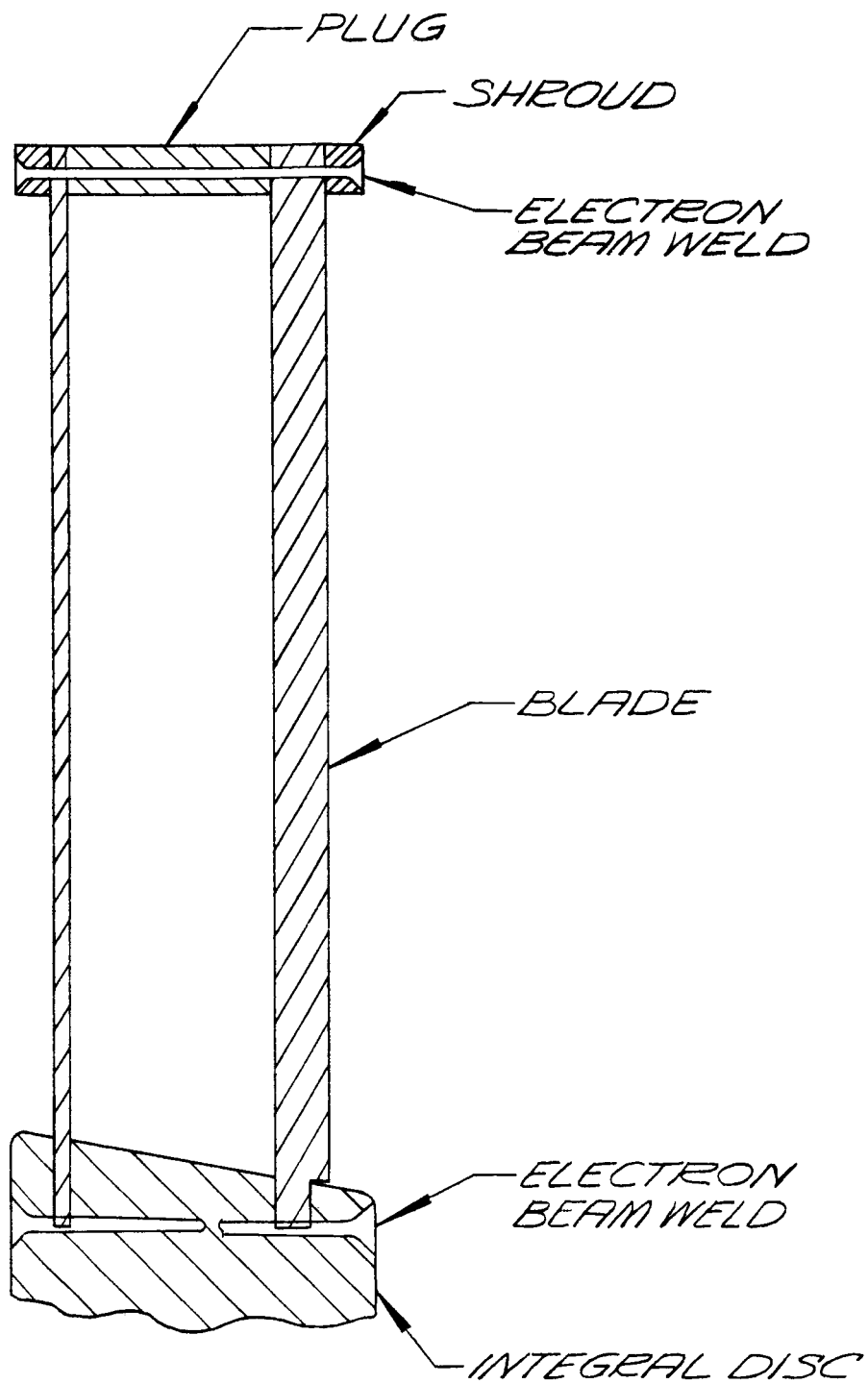
Figure 8

Typical Electron-Beam Weld Configuration

The blades are fastened to the disc and the shroud as previously discussed. The rotor subassembly stage 1 blading has 98 blades that are shrouded in packages of four and five blades each, while the rotor subassembly stage 2 blading contains 94 blades. These are also shrouded in packages of four and five blades each.

2. Nozzle Assembly

This assembly features two solid (one-piece) shrouds which support the 43 nozzle vanes. The assembly itself is supported by the turbine inlet manifold by means of a flange on the outer shroud. Similar thermal growth in the support structure and the nozzle assembly allowed the design shown in Figure No. 3. A thin membrane (0.040-in. thick) supported by the inner shroud ring, and a part of this assembly, provides the closures between the nozzle block and the inlet manifold flange.

3. Reversing Vane Assembly

To accommodate the difference in thermal expansion between the reversing vane assembly and the main casing flange, the reversing vane assembly was segmented into six subsections. These subsections are assembled in a support ring which is shielded from the high gas velocities and high heating rates. The support ring is held in place by the main casing flange of the turbine.

B. DESIGN AND MATERIALS SELECTION

1. Rotor Assembly

a. Requirements

The requirements for the rotor mechanical design were:

(1) Light weight.

(2) No limitation of any aerodynamic features.

(3) Minimum thermal stresses.

(4) Advance in the technology of the manufacturing processes.

(5) Production of 36,000 HP at 4,000 rpm. (This power-speed combination results in low centrifugal but high bending blade forces.)

(6) The turbine drive gases are 90% hydrogen and 10% (by volume) water vapor. The maximum gas temperature is 1000°F and the pressure downstream of the nozzle 100 to 200 psia.

b. Selected Design

The design selected (see Figure No. 2) appears to fulfill the above requirements as follows:

(1) Light weight is achieved through the use of the thin discs which form a box structure and through the use of the hollow blades.

(2) Welding the blades to the disc and the shroud completely eliminated any restrictions upon solidity or axial plan configuration.

(3) The sheet metal blade wall heats uniformly to minimize thermal stresses. The coupling between the hot discs and the cold hub allows relative radial growth of the discs in relationship to the hub.

(4) At the time this design was selected, the butt welding of sheet metal blades into machined slots by electron-beam welding was new. Also, the electron-beam welding process was new and there was little experience with its application to Inconel 718.

2. Stator Assemblies

The requirements for the stator assemblies are identical to the ones for the rotor assembly. A maximum nozzle upstream pressure of 310 psia determines the pressure loads on the nozzle assembly.

The same principles used for the rotor assemblies were again used to satisfy the stator requirements. However, it was found that both the GTAW and EB welding processes were applicable. Initially, drawings for GTAW welded stator assemblies were released. However, similar GTAW welded stator assemblies experienced severe weld shrinkage problems in another turbine designed by Aerojet-General. Therefore, it was decided to apply the electron-beam welding process to the stator assemblies in the same manner as it is used for the rotor assemblies.

3. Material Selection and Material Properties

a. Turbine Component Material Requirements

(1) High strength at operating temperature, which allows thin cross-sections with a corresponding weight saving and favorable thermal stress conditions.

(2) Good elongation at operating and cryogenic temperatures. The turbine gas properties result in very high heat transfer rates to flow passage surfaces. The resulting high thermal stresses require ductile material to prevent surface cracks.

(3) Good weldability because minimum weight construction can be obtained through the use of welded designs.

(4) Good repair weldability in the heat treated condition.

(5) Good machineability.

(6) Freedom from hydrogen embrittlement.

(7) Good resistance to corrosion and oxidation.

b.   Inconel 718

At the time of material selection, there were numerous materials (i.e., A-286 and the precipitation-hardenable stainless steels) for application at temperatures up to 1000°F. Nickel-base precipitation-hardened super-alloys, such as Rene' 41 and Hastelloy R-235, were available for applications in excess of 1400°F. It was found that Inconel 718 appeared to satisfy the temperature range at which the M-1 oxidizer turbine would operate and it satisfied the majority of the indicated requirements. Inconel 718 had good strength and toughness at temperatures ranging from -423°F to 1350°F. It also had good weldability, but its compatibility with the electron-beam weld process was unknown at that time. However, the decisive factor leading to the selection of Inconel 718 was its superior repair weldability (TIG) in the aged condition. This characteristic was considered mandatory in the fabrication of large turbine components.

The Inconel 718 material heat treatment (anneal, age and stress relieve) specifications were developed in parallel with the fabrication of the components.[3] Two heat treatment specifications were developed. The first was an 1800°F solution treatment and 1325°F/1150°F combination aging cycle recommended for stress-rupture controlled applications where notch-ductility is important. This heat treatment is recommended for all high temperature applications. The second specification developed was a 1950°F solution treatment and 1350°F/1200°F combination aging cycle. It is recommended for tensile-limited applications and cryogenic service. The second treatment is superior for assuring age-hardening response in large forgings that have a coarse grain structure.

All material for the rotor and stator assemblies was processed with a 1950°F solution treatment although it might now seem preferable to use material in accordance with the 1800°F solution treatment for the hot turbine components. However, at the time the material was selected, Aerojet-General engineering was using the 1950°F solution treatment for low and high temperature applications. Considering the low nominal turbine operation gas temperature of 730°F, it is evident that the material used to manufacture the turbine components is adequate.

The principal material strength properties of material with a 1950°F solution treatment are shown in Figure No. 9.

C.   ELECTRON-BEAM WELDING PROCESS FEASIBILITY STUDY

As pointed out in the above material discussion, the compatibility of the electron-beam weld process with Inconel 718 was unknown. Therefore, a program using samples was initiated to investigate the feasibility of EB welding the blades to the supporting discs and shrouds.

---

[3]Inouye, F. T., Hunt, V., Janser, G. R., and Frick, V., Summary of Experience Using Alloy 718 for M-1 Engine Components, NASA Report No. CR 54814, 15 July 1966
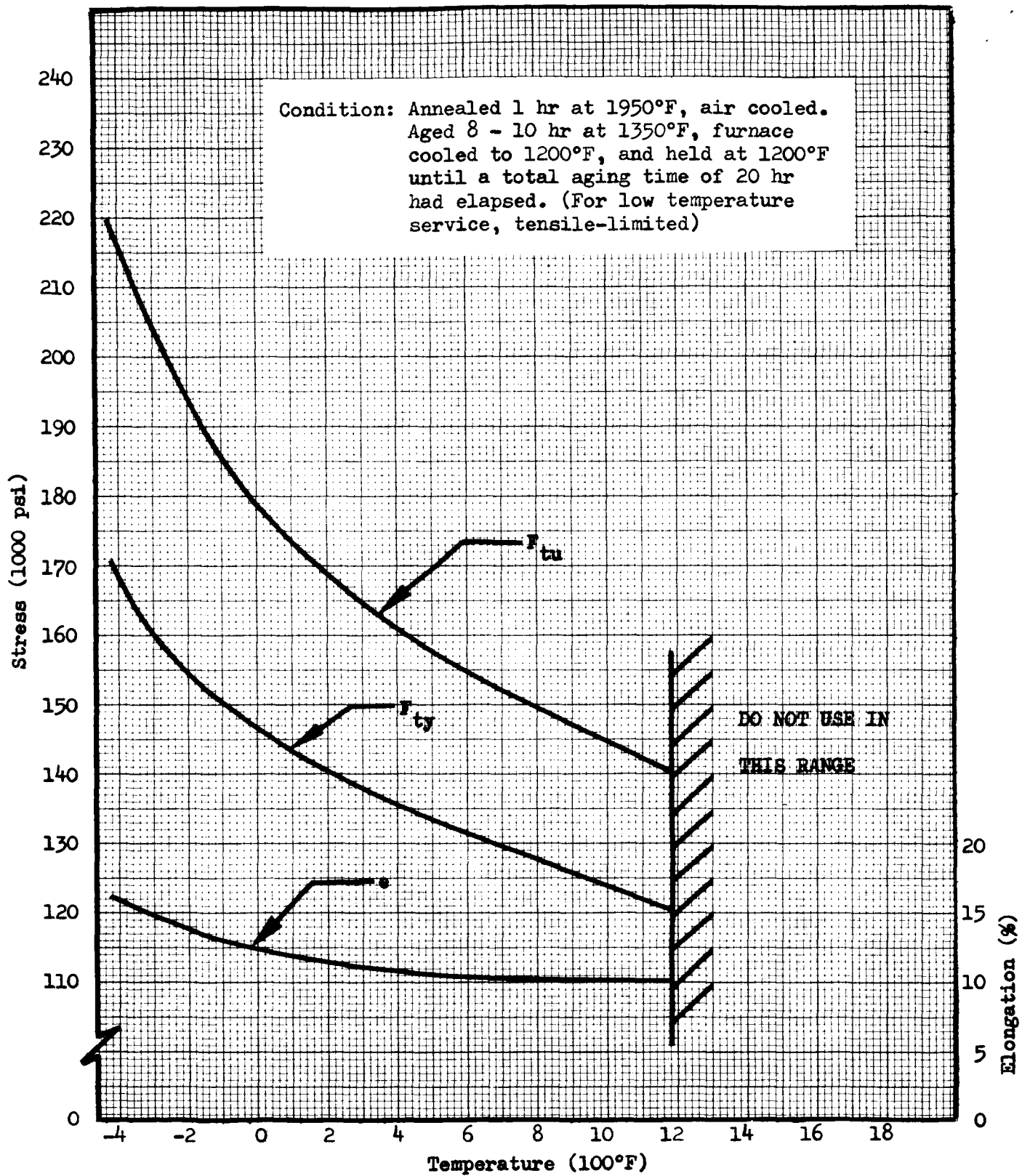
Figure 9

Ultimate Tensile Stress, 0.2% Yield Stress and Elongation vs.
Temperature for Materials of Group 2

Page 14

Concepts for constructing the blade-to-rim joint were investigated early in the feasibility study. In the original design, the blades were welded to a thin rim (Figure No. 10), which formed a conical inner shroud. These subassemblies were then welded to the rim. This design required a three-dimensional programmer because the weld penetration depths varied from the leading to the trailing edge as a result of the blade profile and a conical inner shroud. Figure No. 11 shows a simulated sample utilizing an AISI 347 tube and an Inconel 718 plate, which was welded from the top side in the view shown. Figure No. 11 illustrates the problem of weld depth penetration which varied with the amount of clearance between the tube and the plate.

The design was simplified because of the complicated programming required in the contour weld and the weld penetration problem, although this added some dead weight to the rim. The profile peripheral weld was omitted as shown in Figure No. 12. Weld samples of the blade-to-disc joint are shown in Figure No. 13. In this figure, one sample has been welded from one side only and the other sample was welded from both sides of the simulated disc. Weld samples of the blade-to-shroud joint are shown in Figure No. 14.

Further simplification in the geometry resulted in the final joint configuration shown in Figures No. 15 and No. 16. Weld tests with these samples established a minimum requirement of 0.125-in. distance from the surface to the centerline of the EB weld to prevent erosion such as is shown in the upper view of Figure No. 14. This minimum distance was established based upon the erosion of samples with only a 0.090-in. distance and the successful welds at a distance of 0.125-in.

Samples were fabricated in a tee-shape for tensile testing the butt-weld joint (representing the blade-to-disc joint) and shear joints (representing the blade-to-shroud joint) (see Figures No. 17 and No. 18). A nickel base braze alloy conforming to AMS 4777 (LMW) was applied to one side of the sample to simulate the actual design. Average room temperature tensile strength of the tee-shaped butt weld joints was 174,000 psi with the failure occurring in the parent material. The shear joint failed in the weld at 168,000 psi average stress. The samples were constructed of 0.125-in. plate simulating the blade to assure failure in the weld during the shear tests. The results of these tests gave no indication for concern regarding the use of the thinner 0.063-in. wall thickness material in the actual configuration.

The samples were welded using a weld schedule of a 2.0-in. gun-to-work distance, 50,000 volts, 325 milliampere beam current, and a 6.1 ampere focus current. The speed of travel was 30-in. per minute on specimens welded on one side only and 40-in. per minute on specimens welded from both sides. This weld schedule was used for all samples requiring a contour weld after the original concept.

The braze fillet was added to provide dampening of the blade and vane vibrations. The first braze alloy used consisted of 82% gold and 18% nickel, but it failed to wet and flow properly (see Figure No. 19). The nickel base braze alloy conforming to AMS 4777 (SMW) provided a satisfactory fillet for vibration damping (Figure No. 19). Brazing was accomplished during the heat treatment cycle based upon experience gained with braze test specimens prepared to determine wetability and flow characteristics of the Inconel 718 material. The braze and heat
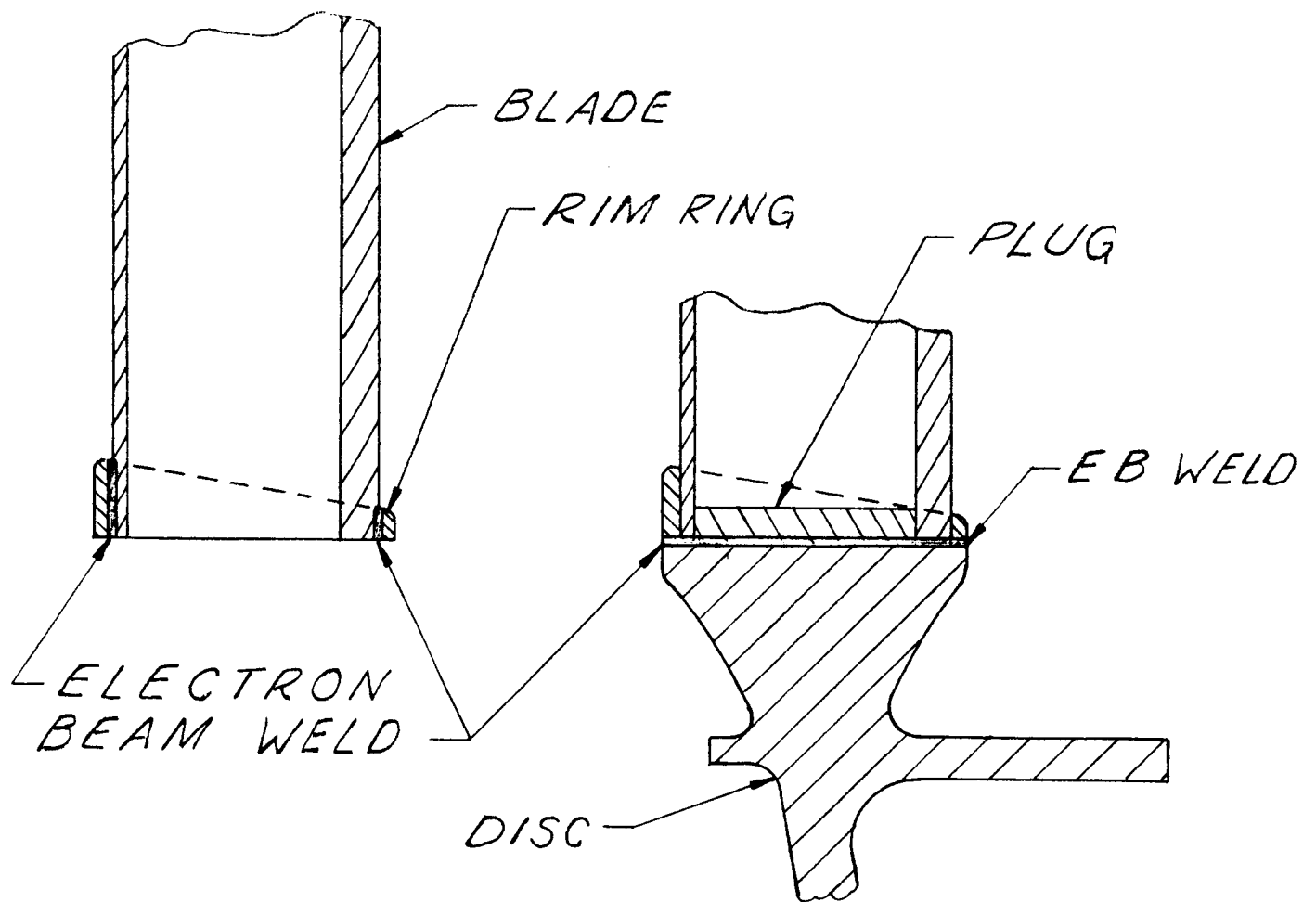
Figure 10

Blade-to-Disc Joint, Radial Contour Weld
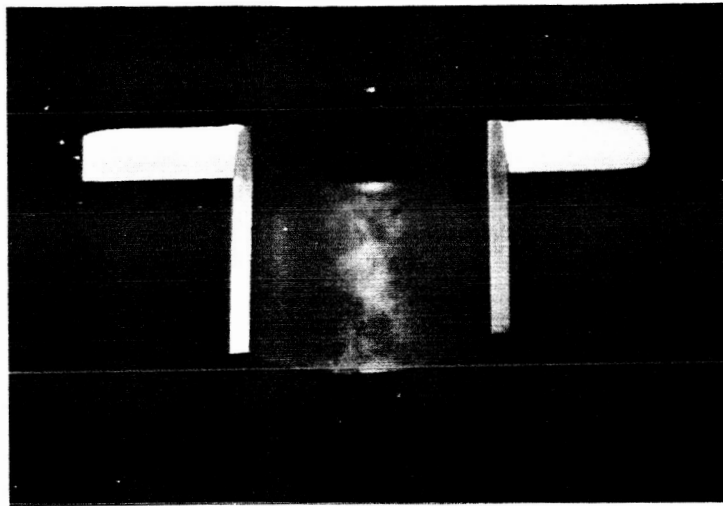
Electron-Beam Weld Joint (Inconel 718 Plate-to-AISI 347 Tube). Depth of weld penetration is directly proportional to the gap width. There was no gap seen on the left weld, while the right weld has a .006-in. gap. This condition was observed under greater magnification of the specimen.
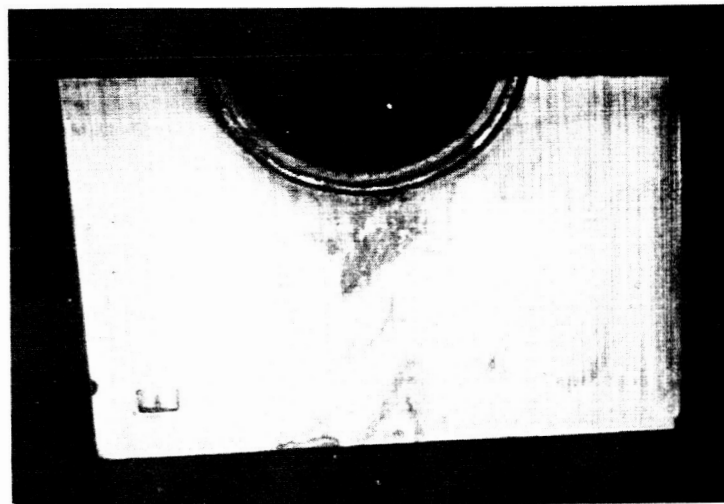
The same specimens show the weld bead resulting from the electron beam impingement which produced the weld seen in the top photo.

Figure 11

Weld Sample Simulating the Radial Contour Weld and Blade-to-Shroud
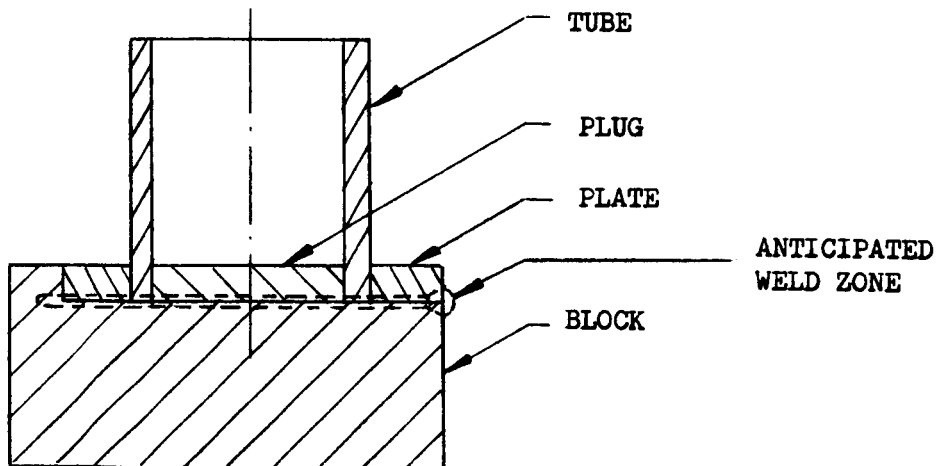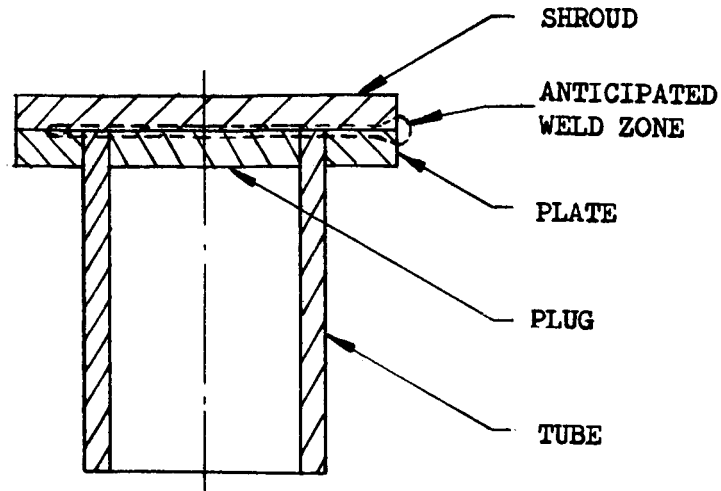
Figure 12

Blade-to-Disc Joints, Axial Butt Joint with Separate Rim Ring
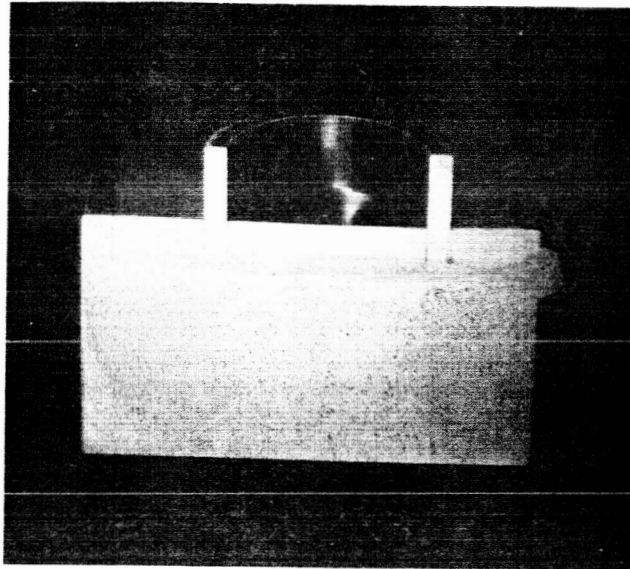
Simulated blade-to-disc joint welded from one side by the electron beam process. Material is Alloy 718.
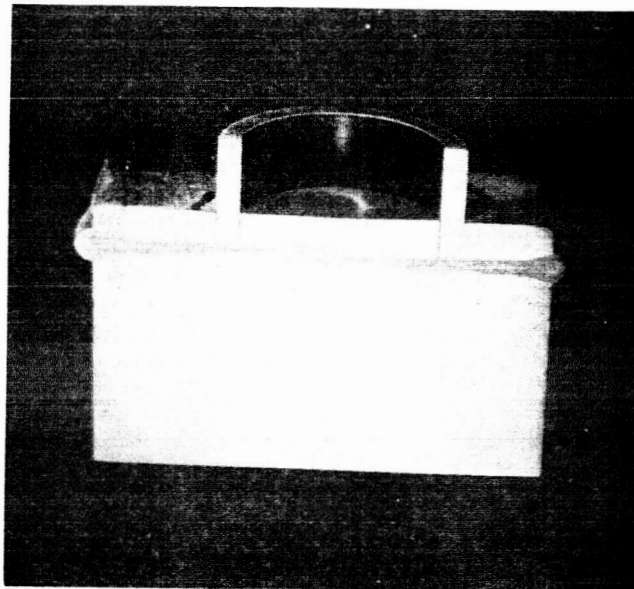
Simulated blade-to-disc joint electron beam welded from both sides and supplemented with a nickel brazing alloy. Base material is Alloy 718; the brazing alloy conforms to AMS-4777 (LMW).

Figure 13

Weld Sample, Axial Butt Joint With Separate Rim Ring
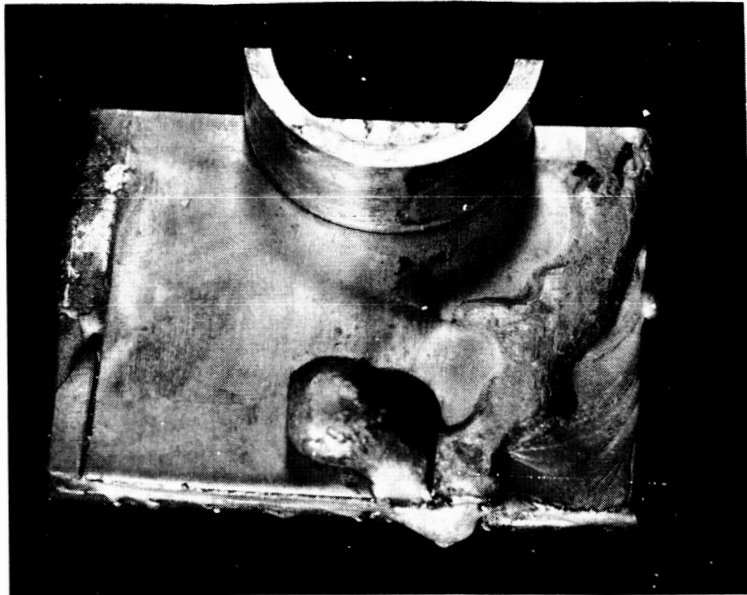
View of the outer blade-to-shroud joint. The thin member (0.090-in. thick) eroded during electron beam welding. All material is Alloy 718.
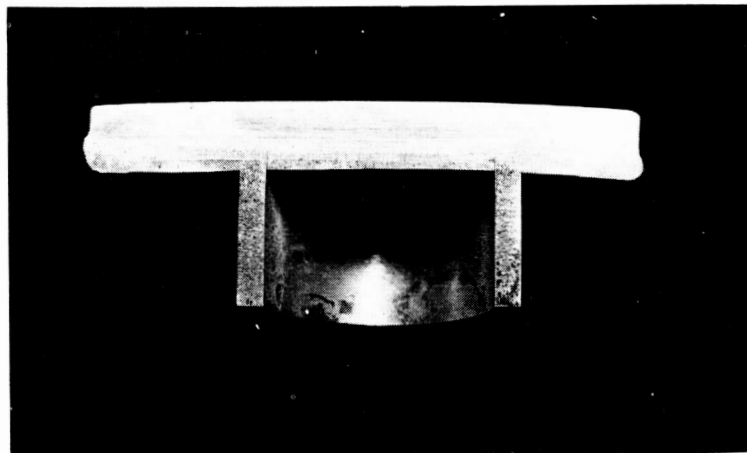
Cross-sectional view showing full weld penetration. The welding was performed from both sides.

Figure 14

Weld Sample, Axial Butt Joint With Separate Ring on Shroud

SHROUD

ANTICIPATED
WELD ZONE

PLUG

TUBE

TUBE

BLOCK

ANTICIPATED
WELD ZONE
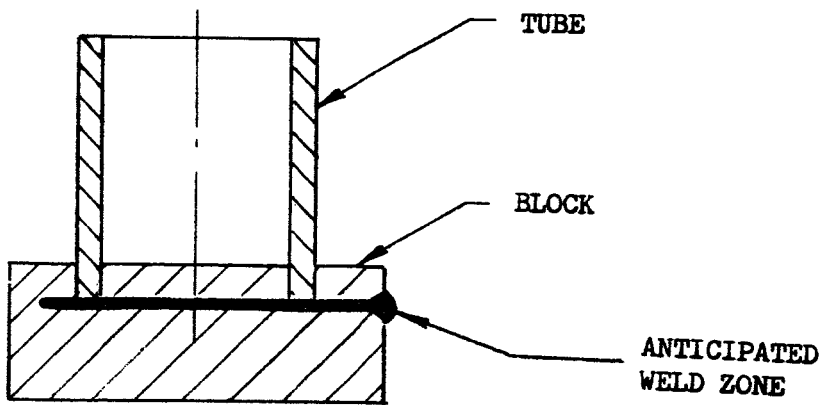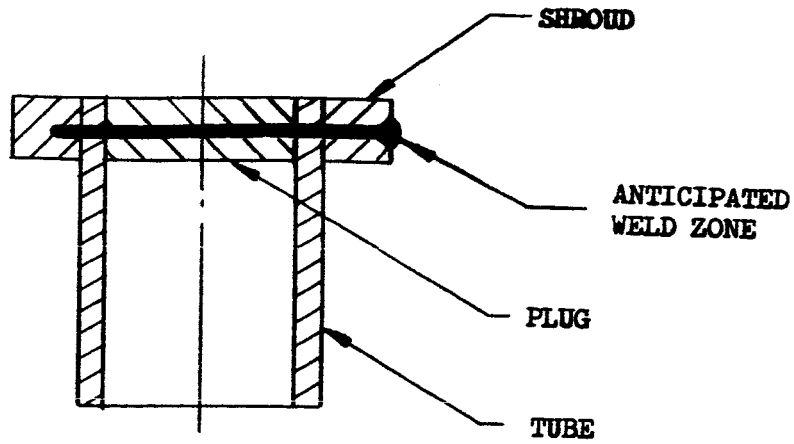
Figure 15

Final Joint Configuration Before Welding

Page 21
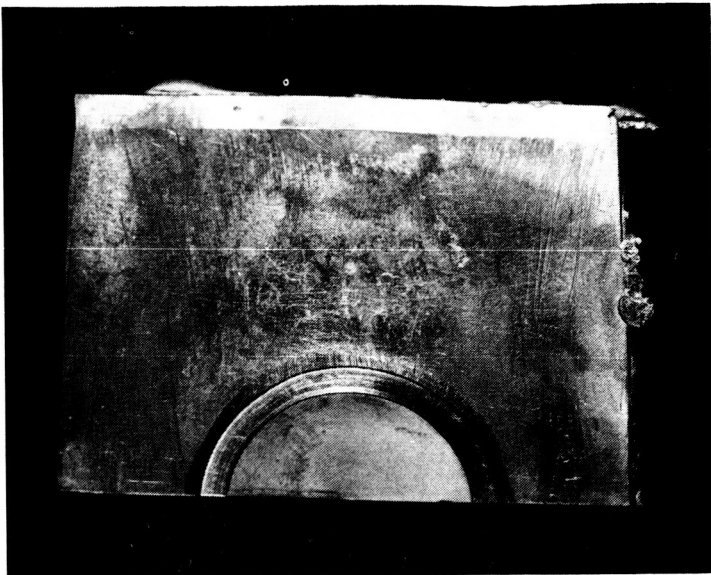
Top view of Alloy 718 tube welded to shroud joint. The tube was plugged to prevent beam deflection and to maintain a constant cross-section area.
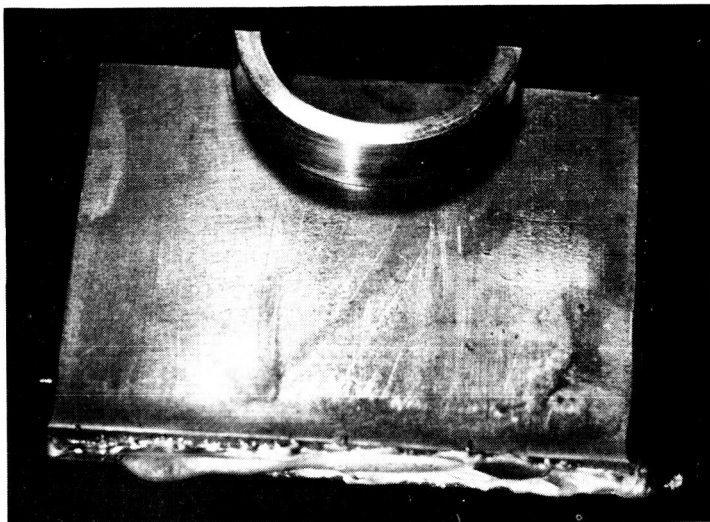
Bottom view of the same joint shows no evidence of erosion or weld burnthrough.
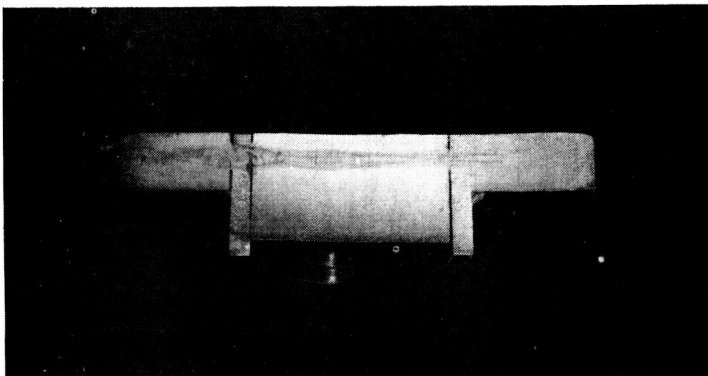
Cross-sectional view of the same specimen shows the weld nugget through the center of the shroud. This specimen was welded from one side only.

Figure 16

Weld Sample, Final Shroud Joint Configuration

.125

BUTT JOINT
FOR BLADE
TO DISC

.125

SHEAR JOINT
FOR BLADE
TO SHROUD
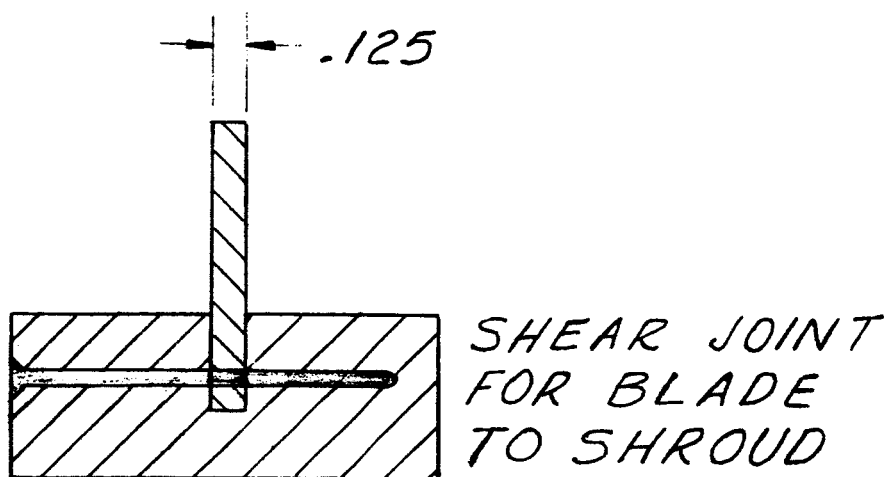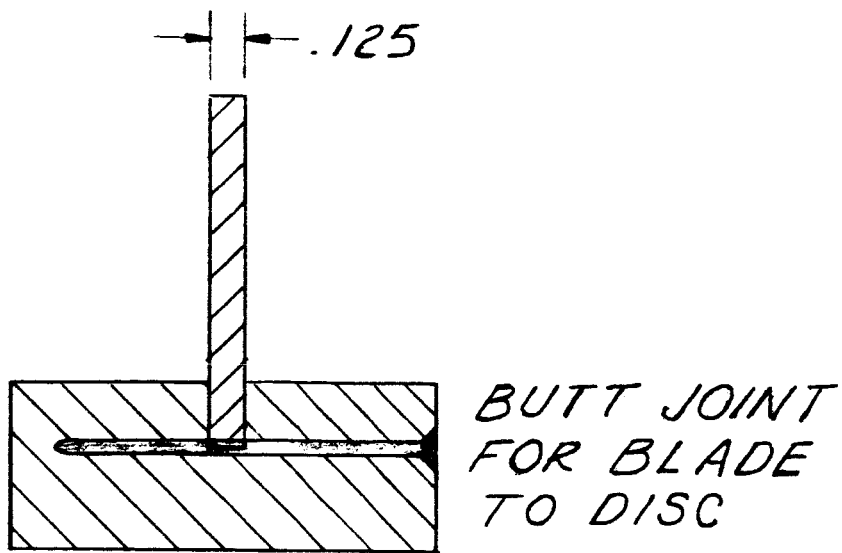
Figure 17

Pull Samples, Final Joint Configurations
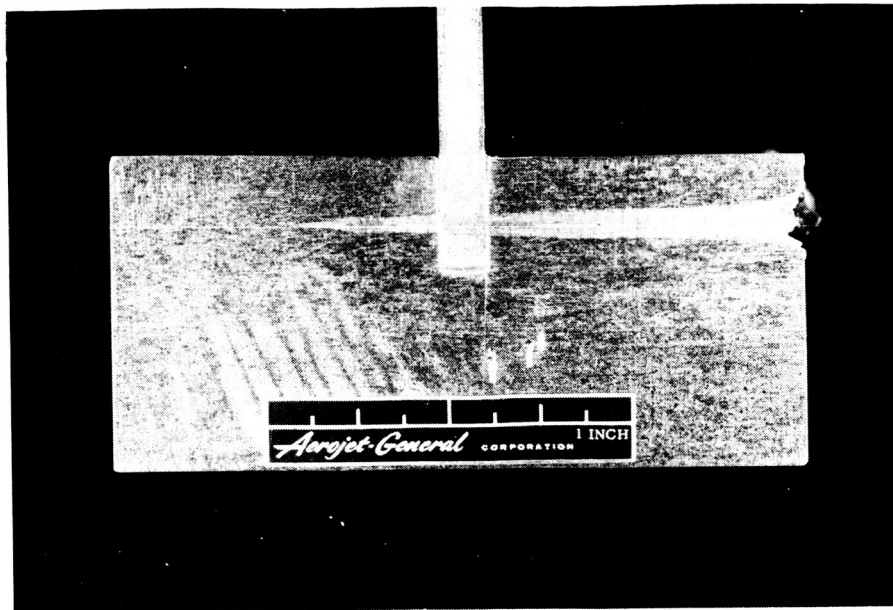
Cross-section view of a T-weld specimen showing the weld nugget
through the blade. The weld specimen has braze on the right side
at the simulated blade-to-disc joint.
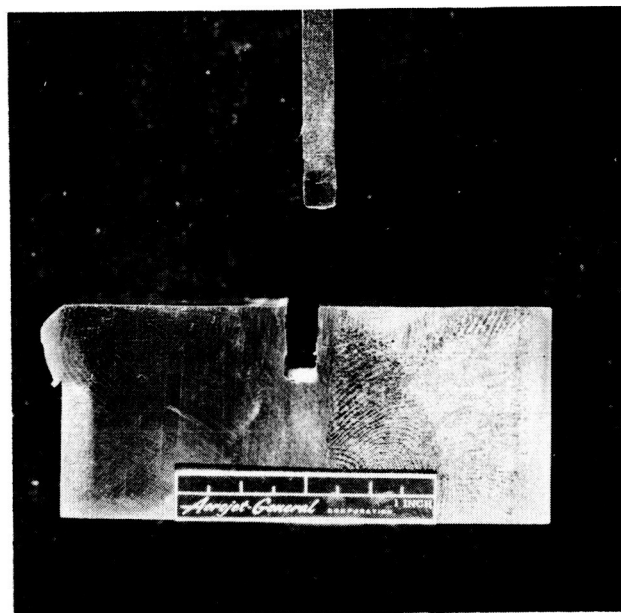
Typical weld shear failure of the test specimen
shown above.

Figure 18

Weld Pull Sample, Final Shear Joint Configuration,
Before and After Tensile Testing
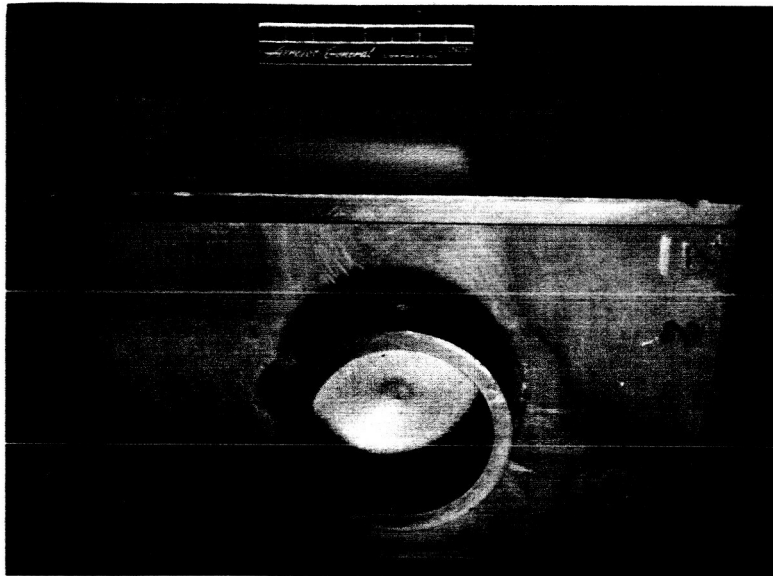
Tube-side of a simulated electron beam welded blade-to-disc specimen after brazing with 82% gold and 18% nickel alloy. Brazing alloy did not wet nor flow uniformly to form a braze fillet.

Same type of specimen shown above except for nickel-base braze alloy conforming to AMS 4777 (LMW). Braze fillet formed uniformly completely around the tube.

Figure 19

Combined EB Weld-Braze Samples

treatment cycle of these specimens consisted of heating them to 1925°F and holding at that temperature for ten minutes in a vacuum. Then, the specimens were air-cooled to room temperature, age hardened at 1325°F for eight hours, and furnace cooling to 1200°F. This was held for a total aging time of 20 hours. Hardness tests conducted with two samples showed a Rockwell "C" hardness of 19.5 to 20.5 before brazing, 19.0 to 26.0 after brazing, and 39.0 to 42.0 after aging. Another specimen was brazed by holding at 1925°F for ten minutes, cooling to room temperature, solution annealing at 1925°F for one hour, then subjecting it to the regular age cycle. Final Rockwell "C" hardness was 39.0 to 41.0. This confirmed that Inconel 718 responds uniformly to heat treatment after both cycles and that the ten minute brazing cycle will provide the solution anneal.

It was concluded that the feasibility of electron-beam welding was demonstrated by obtaining joints with strengths as high as the parent material. These tests also demonstrated that welds could be made without detrimental effects (i.e., microfissures, which subsequently became a problem and which are further detailed in this report). The feasibility study confirmed that Inconel 718 could be brazed satisfactorily and a separate solution anneal after brazing was unnecessary.

D. FABRICATION OF COMPONENT PARTS

All the development work reported in this section was performed by the Jet and Ordnance Division of Thompson-Ramo Wooldridge (TRW), Incorporated of Cleveland, Ohio.

1. Rotor Blades and Nozzle Vanes

The profiles are two piece constructions consisting of a formed sheet metal section and a trailing edge section. The two sections are joined together by electron-beam welding, and the heavy trailing edge section is milled and ground to the final blade configuration (Figure No. 20).

The sheet metal section of each profile is formed in multiple form dies in five steps. The sheet metal sections were stress relieved after the fourth and fifth forming steps. Considerable die development and two stress relieve cycles were necessary to overcome the "spring-back" in the relatively unknown Inconel 718.

The formed and square ended sheet metal portion of the blade as well as its rectangular trailing edge section are assembled in the EB weld fixture with a gap between the two parts of less than 0.0015-in. A 0.060-in. diameter weld wire, placed over the beam exposed side of the weld joint, provided weld reinforcement on this side, while weld drop-through provided weld reinforcement on the other side. This technique eliminated weld "suck-down" and voids. Figure No. 20 delineates the weld schedule used for both the rotor blades and the nozzle vanes. This joint is discussed further under Section III, E, 6, e of this report.

The trailing edge section of the welded blade is milled, ground, and faired to its final configuration. Then, the blade is machined to length as part of the preparation of the blade-to-disc interface.

OPERATIONAL SKETCH

ATTACHMENT 1

DO NOT SCALE DRAWING

TOLERANCE ON DIMENSIONS UNLESS SPECIFIED ARE ±

⊕ GRINDS ORL USED BY THOMPSON

40120L-00

Schedule Number EB-2-7469-4A   Date: 2/8/65
Circumferential Weld   Longitudinal Weld ✓
Mfg. of Machine Zeiss   Material Type INCO-718
Mfg. Serial No. 331   Component Parts PN's. 40139-00
Tapco or Gov't. Serial No. TP-24698   40135-00
Type of Machine ELECTRON BEAM   Assembly Part No. 40135-00
Machine Capacity, KV 60 MA 500   Customer's Name AIRCRAFT GENERAL
Type of Joint SQUARE BUTT   Applicable Spec. 1-54-1655
Bay Location B-17   Plant Location TAPCO

High Voltage, Initial 15 Final   Gun to Work Distance 5"
Slope Rate   Filament Size 500 MA
Milliamperes, Initial 175 Final   Filament To Ca.Dist. 381
High Voltage Start Delay or Tack Weld-   Spacer
 , Range Rate   Anode "Type" 500 MA
Motor Start Delay, X , Range,   Cathode "Type" 500 MA
Focus Pot."Ref."82 Meter "Amps".10   Angle of Gun to Wrkpc. 90°
Filament Current 55-58   Power Supply Freqency 60 Cycle 440 V
Movement of Part(IPM)-Pot Act.   Filler Alloy Type INCO-718
Gun Travel(IPM)-Pot 23 Actual 21   Rod Diameter .060
Direction FORWARD   Rod Feed

Wire stationary on piece part.

Weld Engineer:
Laboratory:
Quality Control:

.063 SHEET METAL SECTION
.060 DIA, FILLER WELD WIRE
ELECTRON BEAM WELD
TRAILING EDGE SECTION

Thompson Ramo Wooldridge Inc.
CLEVELAND, OHIO

OPER DESC

TITLE
BY NAME Aero-Jet General
MACHINE TP 24698
DRN TDZ DATE 2/4/65
CKD MCN DATE
ALTERNATE SKETCH

DATE & SIG   RECORD OF ALTERATIONS
REC'D BY

Figure 20

TRW Operational Sketch, Weld Schedule for the Rotor Blades
and the Nozzle Vanes

The contour of the airfoil was inspected using a guillotine gage and the integrity of the EB weld joint is verified through X-ray and dye penetrant inspection.

2. Preparation of Rotor Discs and Shrouds, and Stator Shrouds

The rotor discs and shrouds as well as the stator shrouds were rough-machined and approximately 0.10-in. of stock was left for final machining with the following exceptions:

a. The outside diameter of the rotors and the inside diameter of the outer stator shrouds were final machined in preparation for the cutting of the profile slots.

b. The inside diameter of the rotor shrouds and the outside diameter of the inner stator shrouds were machined to 0.050-in. stock on the diameter in preparation for cutting of the profile slots. These small amounts of stock were left to allow for adjusting the blade throat area, which is accomplished through adjustment of the blade-height (H) before welding.

During the early phases of the EB weld feasibility program, the gap between blade and disc became a parameter of major importance. The penetration of the electron-beam was considerably reduced if the beam had to travel through significant gaps. A maximum gap of 0.008-in. was allowed between the disc and the blade, and the blade and the plug. This was based upon tests made with varying gaps. Because of variations in blade/vane geometry, it was necessary to custom cut each slot for a given blade as described in the ensuing discussion. Further, the EDM energy output had to be adjusted for electrode erosion during the cutting process.

The tooling for the EDM machining of the profile slots consists of basic holding and indexing fixtures, and roughing and semi-finishing carbon electrodes. These electrodes are true copies of the blades, cut on a duplicating machine from the serialized blades or vanes. Each blade end was copied on a cutting electrode and had its custom fit slot in the shroud or disc. Figure No. 21 shows such an electrode. All of the slot cutting was done on Cincinnati Electrical Discharge Machines.

Prior to machining of the slots, a map was compiled for positioning the rotor blades by weight and airfoil geometry. The weight consideration minimizes out-of-balance conditions in the finished assembly and the airfoil geometry is used to establish the total required throat areas for rotors and stators. After discs or outer stator shrouds were installed and indexed in the holding fixture, a roughing cut was made with the carbon electrode to approximately 0.030-in. of the required depth. Then, the electrode was dressed for the semi-final cut to 0.010-in. of the required depth. For the final cut, the mating blade itself was used as the tool to cut the slot to its final depth. This gives an almost zero gap butt joint between the blade and the disc (or vane and shroud). This three-step procedure was followed for each butt joint to achieve a tight fit with a minimum gap between parts.
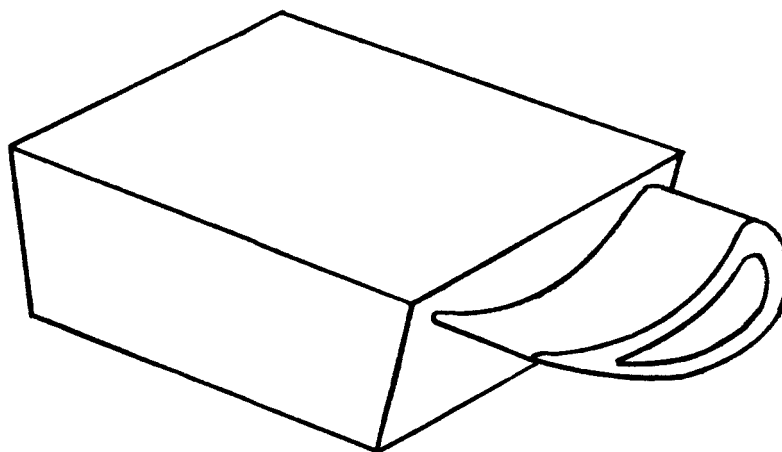
Figure 21

Slot Cutting Electrode for Rotor

Page 29

E.   DUMMY ROTOR PROGRAM, ELECTRON-BEAM WELD DEVELOPMENT

   1.   Justification

         The EB weld feasibility program had been conducted under laboratory
conditions at the facility of an EB weld machine manufacturer. The samples were of
simple geometrical shape, allowing good gap control, and small in absolute dimensions.
The material was randomly selected Inconel 718 and stainless steel.

         It appeared mandatory to develop proper techniques using prototype
samples at the vendor facility and for his welding machine. Further, the actual
complex profile shape was to be used to determine gap effects. The blades were to
be prepared by the same processes as would be the final blade. The test slots were
to be cut by the EDM process rather than milling, which is significant because the
EDM process shows Laves Phase surface irregularities if Laves Phase is present in the
material. Conventional machining, such as milling and grinding, results in a metal
surface smear which covers the small Laves Phase surface imperfections giving the
appearance of a smooth surface without any apparent defects. Material that was
representative of the heats of the material for the actual hardware was to be used.
Brazing was to be attempted with prototype material and cleanliness levels identical
to the ones for the prototype hardware. Finally, pull samples of the actual joint
configuration were to be obtained.

         It was questionable whether X-ray inspection would provide con-
clusive information about the quality of the blade-to-disc and blade-to-shroud
weld joints. For this reason Aerojet-General regarded it essential to award a
contract to the Thompson-Ramo-Wooldridge Corporation for the purpose of proposing
and developing inspection procedures using dummy rotors.

         Uncertainty in the stress and vibration analysis of the rotor blade
packages indicates a desirability for experimentally determining the natural frequen-
cies of rotor blade packages consisting of four and five blades.

         Three dummy rotors were ordered from the vendor; two of these
dummies to simulate the configuration of the second-stage rotor and the remaining
dummy to simulate the first-stage rotor. Figure No. 22 shows these dummy rotors.
One dummy of each configuration was used to establish the natural frequencies of
the blade packages. The second stage-two dummy was cut up to evaluate weld joint
configuration and weld joint integrity. This was also done to establish inspection
procedures and to machine pull samples. Lastly, the dummy rotors provided an
opportunity to test tooling that was identical to that intended for the prototype
hardware. Aerojet-General awarded a contract to Thompson-Ramo-Wooldridge to
evaluate the dummy rotor. The results of this evaluation have been reported
elsewhere[4] and are summarized in the following discussions.

---

[4] Kane, R. F., Aerojet-General M-1 Oxidizer Program, Evaluation of Second-Stage
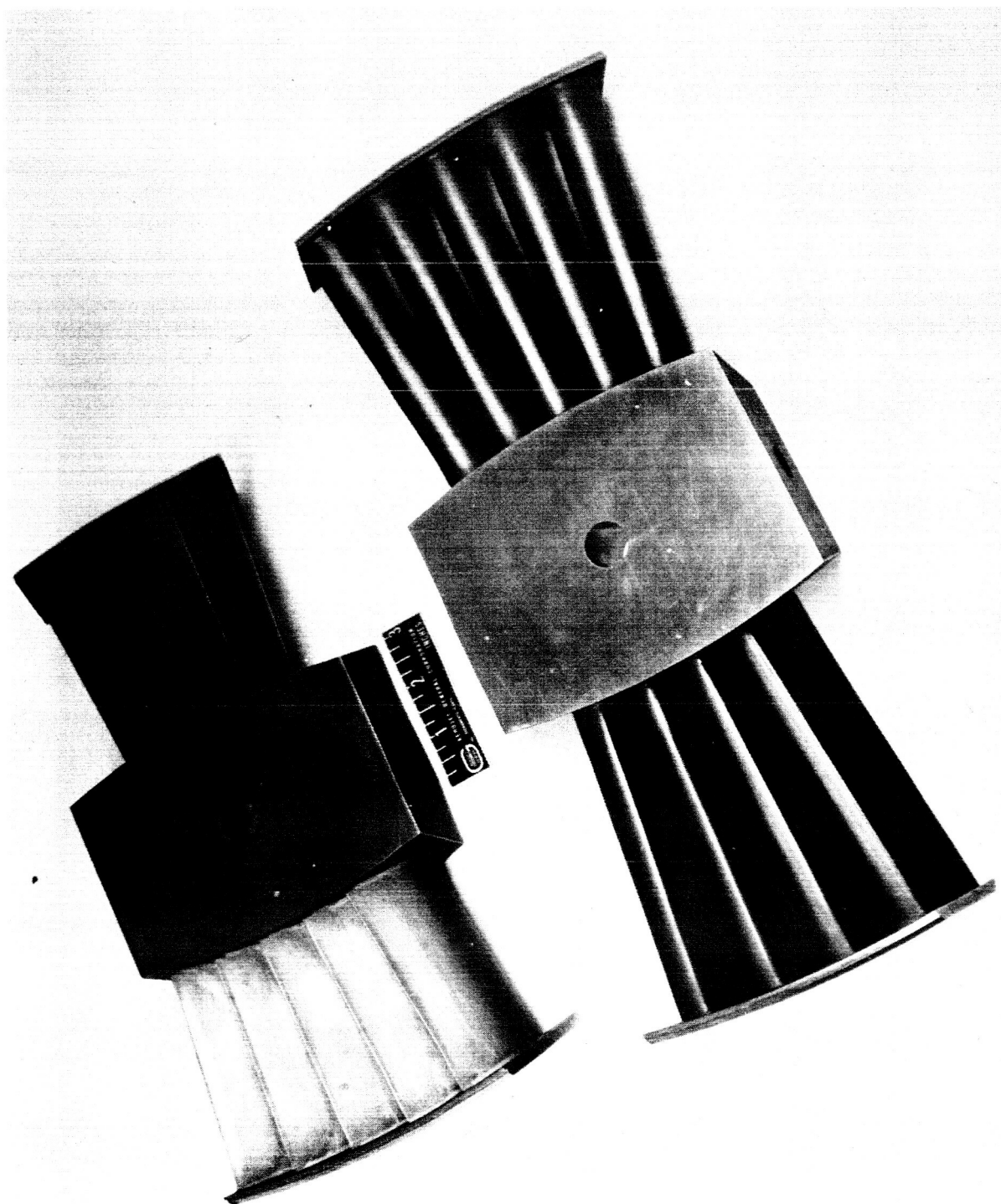   Dummy Rotor, S/N 1, Thompson-Ramo-Wooldridge, Inc., May 1965

Figure 22

First-Stage and Second-Stage Dummy Rotors

2.   Pre-Dummy Rotor Weld Development

Prior to welding the first dummy rotor, Thompson-Ramo-Wooldridge conducted an extensive weld development program using the weld samples shown in Figures No. 8 and No. 23. Microfissuring was encountered in most weld samples.

The microfissures were intergranularly perpendicular to the weld and associated with eutectic melting in the grain boundaries of the parent material immediately adjacent to the weld. Tests indicated that this micro-cracking was dependent upon the electron-beam weld schedule. A high voltage, rapid speed weld schedule tended to result in the least amount of microfissuring. The electron-beam gun-to-work distance also appeared to be critical; the closer the gun was to the work, the less severe was the microfissuring in the nail head and the shank of the electron-beam weld. Fixturing accessibility made it necessary to use a 3.5-in. gun-to-work distance as compared with the 2.0-in. distance used during the electron-beam welded feasibility studies.

The mill heat of material also appeared to have an effect upon the severity of the microcracking. Some heats of material examined during the period of weld schedule development showed no signs of cracking while others cracked quite severely. A smaller grain size material also appeared to reduce the amount of microcracking. For this reason, the 1750°F solution anneal material could possibly be better suited for electron-beam welding than the 1950°F anneal condition because the lower solutioning temperature is more conducive to a finer grain size material.

The microfissuring was most severe in the area of the nail head (see Figure No. 23) where some fissures were 0.030-in. long. Along the stem, a fissure length of 0.005-in. was found. Microfissures existed, in some cases, every 0.030-in. to 0.050-in. along both sides of the nail head and the stem. Figure No. 24 is an enlargement of a typical section of a weld sample.

Samples of the type shown in Figure No. 8 displayed not only microfissuring but also porosity in the molten zone. This porosity was attributed to inadequate cleaning of the blade and the slot before assembly.

3.   Manufacturing of Dummy Rotors

The dummy assemblies were fabricated using prototype blades and sections of prototype outer shrouds from the reversing vane assemblies. The disc portion of the assembly was simulated by using a nearly-rectangular block of material approximately six-inches long, four-inches wide, and two-inches thick. The center hub section was machined to hold five blades on one side and four blades on the other side.

The dummies were fabricated entirely from Inconel 718 material purchased in the 1950°F anneal condition in accordance with Aerojet-General Specification AGC-44152 with respect to the sheet stock and AGC-44151 with respect to the bars and forgings. Because double vacuum melted material was reported to be more suitable for electron-beam welding as it is less susceptible to "blow holes" occurring in the weld, all forging material purchased was of the double vacuum melted type.
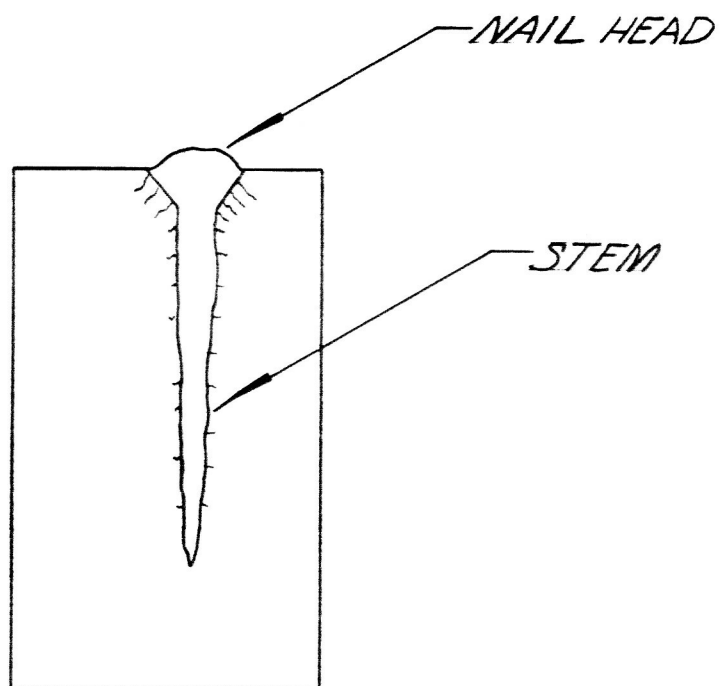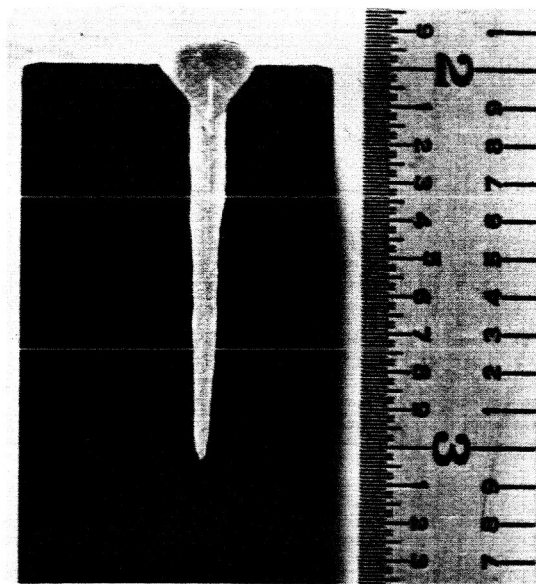
Figure 23

Weld Sample and Schematic of Microfissure Pattern

MAG: 50X

Figure 24

Photomicrograph Showing Microfissuring on Typical Nail Head

The slots for the blades were cut into the disc and shroud section in a manner identical to the prototype discs.

Because of porosity problems in the electron-beam welds as well as a light oxide tint on the electrical discharge machined surfaces of the hub, shroud plugs, and outer shroud, it was necessary to pickle the components in a ferric chloride solution prior to welding to remove all surface contamination. Operating temperature of the solution was 105°F. After a normal pickling time of five minutes, the components were withdrawn from the pickling tank and rinsed in hot water. A visual examination of the EDM surfaces revealed them to be covered with a black coating which would not wet and caused defects in the EB welds. After removing the coating with a stream spray, the components were repickled. Because the black coating reappeared, pickling times approaching 20 minutes were found necessary to obtain a contaminant-free EDM surface. The composition of the black coating was not determined.

The blades were originally cleaned using a dry glass bead blast to remove the oxide formed in the stress relieving operation. Pickling was not used because there was a danger of trapping acid in the trailing edge of the blade. A severe porosity condition in the outer shroud electron-beam weld on the first dummy was found and it was necessary to polish the areas of the blade to be welded with a carbide burr tool. Spectrographic analysis showed silica on the surface of a blade cleaned by the dry glass bead blast method. It is possible this silica deposit contributed to the porosity problems encountered with the first dummy. Subsequent parts that were welded after the blades had been polished with a carbide burr tool showed a significant decrease in the amount of porosity present in the weld.

The dummy was assembled into the prototype welding fixture and the blades were electron-beam welded to the hub at the base of the blade slot. The blades, shroud plugs, and outer shroud were joined by an electron-beam weld through the outer shroud located approximately 0.100-in. from the inner edge of the outer shroud.

Each weld joint was welded with two passes, one on each side of the part. The penetration of the first pass was regulated to give slightly greater than 50% penetration; the part was then turned over and the same weld schedule was applied to this side. Because the two passes were made at the same diameter, 100% weld penetration resulted. Figure No. 25 is the electron-beam welding schedules used for the dummy assembly. The weld sequence required three chamber evacuations. First, the hub section of the trailing edge side was welded; then, the part was turned around and the disc and shroud sections, in that order, were welded on the leading edge side. Finally the part was again turned and the shroud section was welded on the trailing edge side. This weld sequence was necessary to minimize distortions.

After welding the first dummy, a section containing a blade welded to the hub and the outer shroud was cut from the assembly for microexamination. This section is shown in Figure No. 26. The remainder of the dummy was radiographically inspected and gas leaked checked as described in Section III,E,4,a of this report.

 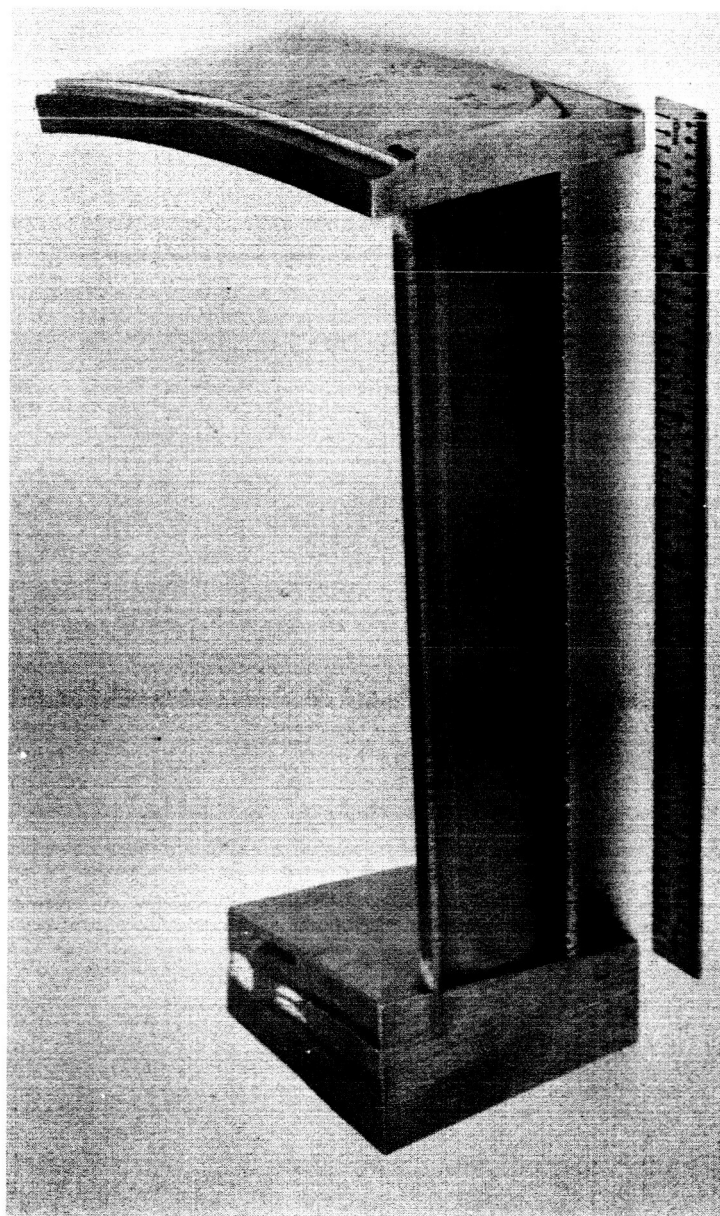
Trailing Edge
E. B.
E. B.

ANGULAR TOLERANCES UNLESS SPECIFIED ARE ± DO NOT SCALE DRAWING TOLERANCE ON DIMENSIONS UNLESS SPECIFIED ARE ± DRAWING USED BY THOMPSON

OPER. NO. 941-111

F.R. NO. 401251-00

401251-00

Schedule Number #B-24683-5A	Date: 5/4/65
Circumferential Weld X	Longitudinal Weld
Mfg. of Machine Sciaky	Material Type Inco 718
Mfg. Serial No. 8387	Component Parts PN's. 401278-00
Tapco or Gov't. Serial No. TP-24688	401254-01, 401256-00
Type of Machine Electron Beam	Assembly Part No. 401275-00
Machine Capacity, KV 60 MA 500	Customer's Name Aerojet General
Type of Joint Bead on plate,	Applicable Spec.
Bay Location G-12	Plant Location Tapco

High Voltage, Initial 40 Final 50	Gun to Work Distance 3.500"
Slope Rate 3	Filament Size 500 MA
Milliamperes, Initial 300-320 Final	Filament To Ca. Dist. .383
High Voltage Start Delay or Tack Weld-	Spacer 350 MA
%, Range, Rate	Anode "Type" 60 KV
Motor Start Delay. % 15, Range,	Cathode "Type" 500 MA
Focus Pot. "Ref." 324 Meter "Amps". 5.6	Angle of Gun to Wrkpc. 90°
Filament Current 55 - 58	Power Supply Freqency 60 cycle, 440 V.
Movement of Part (IPM)-Pot 2.0 Act 53.5	Filler Alloy Type
Gun Travel (IPM)-Pot Actual	Rod Diameter
Direction Right	Rod Feed

age #2, "O.D."

Weld Engineer: James C. Knoefel

Laboratory: E. F. Kane

Quality Control David Francis

Thompson Ramo Wooldridge Inc.
CLEVELAND, OHIO

CODE

OPER. DESC.

TITLE

MAT'L. Inco 718

CUST. NAME Aerojet General

CUST. PT. NO.

MACHINE TP-24688

LET	WAS	DATE & SIG	REC'D. BY

RECORD OF ALTERATIONS

DO NOT ALTER THIS D.P. WITHOUT FIRST SENDING CHANGE SLIP TO ENG. DEPT.

DR'N JOK DATE 5/4/65

CK'D HJN DATE 6/-/65

ALTERNATE SKETCH

F.R. NO.	OPER. NO.
401251-00	941-1111

Figure 25

TRW Operational Sketch, Weld Schedule for the Dummy Assembly

Figure 26

Close-Up of the Vane Section Removed from the Second-Stage
Dummy Assembly After Electron-Beam Welding

The dummy was cleaned with acetone and prepared for brazing by applying Nicro braze, type LMW, around the blade-to-hub/and outer shroud joints. This braze alloy, which has a proprietary additive, was originally developed for brazing in a marginal argon-type atmosphere. Experience at Aerojet-General has shown that the additive also improved wetting and flow characteristic in vacuum brazing operations

The assembly was vacuum brazed at 1 to 5 microns, at a temperature of 1900°F to 1950°F for 10 to 12 minutes and cooled to room temperature with a circulated argon atmosphere. Appendix A is a copy of the brazing procedure.

The dummy was then aged in accordance with AGC-46604; 1350°F for 8 to 10 hours, furnace cooled to 1200°F, then held at 1200°F until a total aging time of 20 hours had elapsed (see Appendix B for the aging procedure). The assembly was then machined in accordance with the blueprint requirement, Zyglo inspected, and sent to the laboratory for testing.

4.   Development of Non-Destructive Test Procedures

The following test procedures were developed in this program

a.   Gas Leak Check

The gas leak check was used primarily to determine nondestructively whether the electron-beam weld fused the end of the blade completely to the hub and had not passed through the hub, thereby missing the blade.

To perform this check, a small tube was first inserted into one of the two 0.062-in. diameter vent holes in the blade. This tube was sealed to the blade by the use of Apizon "Z" sealing compound. A Veeco Leak Detector, Model MS-9AB, was used to pump the blade cavity down to 10^{-3}mm pressure. Helium was then sprayed around the blade-to-hub and blade-to-outer-shroud joints to check for leaks. If a leak is present, helium enters the vacuum system and the mass spectrometer indicates its presence. The location of the leak is pinpointed by pressurizing the blade and applying soap bubbles to the questionable area. Each blade in the dummy rotor assembly was separately tested in this manner.

b.   Radiographic Inspection

Radiographic inspection was used to determine the location of the electron-beam weld in the hub as well as to determine weld quality. The dummy was radiographed using a 300 KV Norelco unit with a 4.0 mm focal spot. The films were exposed at 290 KV - 10 mm at a 24-in. focal-film distance for 13 minutes. A 0.005-in. lead screen was used in the front and back of the cassette with no filtration at the port. The X-ray beam was centered over and parallel with the welds on both the hub and outer shroud. To determine the extent of the porosity conditions found in the outer shroud weld, additional exposures were made at approximately a 45 degree angle to the weld in the outer shroud.

c.   Zyglo Inspection

Penetrant inspection was performed after final machining in accordance with AGC-STD-4816, Type I, Class 2. The assembly was dipped into ZL-1C penetrant oil and allowed to drain for one hour. After washing with warm water, the part was dried at 150°F to 180°F. Inspection was performed after applying ZP4 dry developer. Development time was controlled from a minimum of 10 minutes to a maximum of one hour.

5.   Destructive Test Procedures

a.   Preparation of Metallographic Specimens

The blade segment removed from the dummy assembly after welding was sectioned to produce metallographic specimens showing the electron-beam weld in the hub, the outer shroud, and the blade. All specimens were polished and examined in the unetched condition and then again after etching. Additional metallographic specimens were taken from the hub and outer shroud electron-beam welds after brazing, aging, and final machining.

b.   Mechanical Testing

The outer shroud from the four blade side of the dummy was cut between each blade. The blades were then relieved from the hub by a chevron shaped cut between the blades. A 1/2-13 tapped hole was machined into the vane base and an adaptor fixture was made to grip the shroud end of the vane. Three blades were tested in tension on a 60,000 lb Baldwin-Lima-Hamilton hydraulic tensile testing machine. When the outer shroud sheared from the vane, the shroud plug was tapped to accept a 3/8-16 stud. The plug sheared from the vane during retesting. Testing was then continued using one blade by gripping the blade end in flat jaws. Figure No. 27 shows the testing fixture and a tested blade.

6.   Results of Testing

a.   Gas Leak Check

The primary purpose of the gas leak check was to determine whether the electron-beam weld actually intersected the blade and the base of the blade slot in the hub. The blueprint required that the weld must pass through the end of the blade at the base of the blade slot and concern existed that the weld may have missed the blade entirely and lie totally in the hub. Because the weld at its center is only 0.050-in. wide and is centered on the theoretical diameter indicated by the base of the blade slots, the margin for error is only half the weld width, or 0.025-in. Therefore, the total tolerances, including the depth that the slot, the bottoming of the blade into the slot, and the radii at the base of the EDM slot, all must fall within a 0.025-in. tolerance.

If the electron-beam weld misses the intersection of the blade and the base of the slot, a very severe gas leak would occur when tested either under vacuum or positive pressure. When helium leak tested on a mass
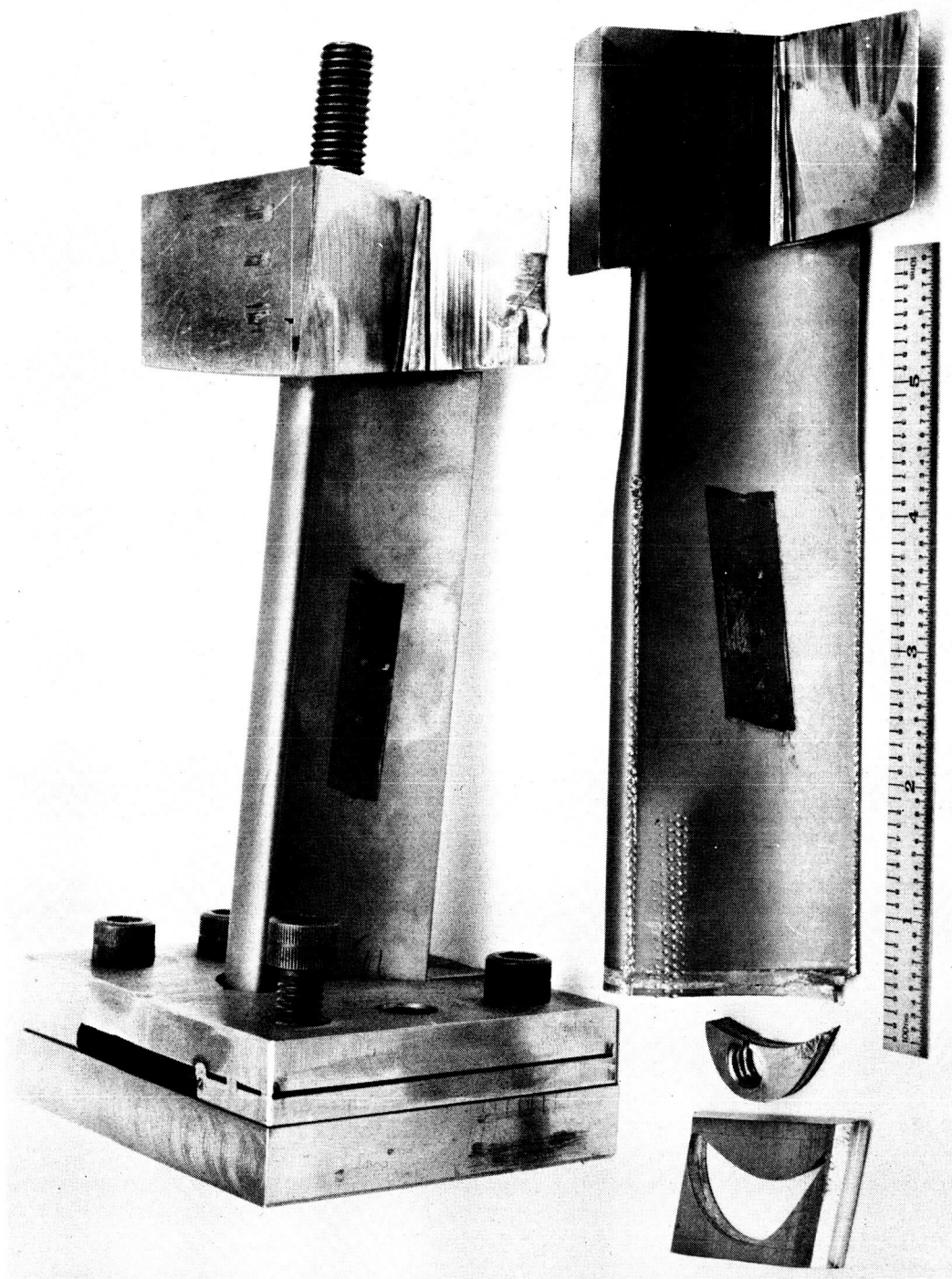
Figure 27

Test Fixtures for Tensile Testing of Blade Samples

Page 40

spectrometer, the dummy showed no leaking whatsoever in the blade-to-hub weld. However, gas leaks were found in the outer shroud area on two of the eight blades tested. The leaks were pinpointed by spraying acetone on the blade area under vacuum and also by applying a soap solution on the part with the blade under a positive pressure. The leaks were found in the outer shroud plug-to-blade weld. In both cases, the leaks were at the leading edge of the blade intersection with the shroud plugs.

The other two mock-ups were tested and similar leaks were found. A visual examination of the outer shroud in this area revealed, in most cases, a rather large gap at the outer shroud-to-blade intersection. This gap appeared to be approximately 0.025-in. in width and the result of weld shrinkage. Because only the blade was pressurized, it was not determined whether a leak existed at the leading edge intersection of the blade-to-shroud.

b. X-Ray Inspection

The radiographic evaluation of the dummy assembly gave a good indication of the amount of porosity present in the weld. However, a super-position effect was noted on the radiograph of the outer shroud weld of the first dummy. In this radiograph, which was taken parallel to the weld, a dark indication approximately two-inches long and as wide as the weld was observed. In an effort to determine the nature of this indication, another exposure was made at a 45 degree angle to the weld. Figure No. 28 is a photograph of the X-ray film. The two-inch long indication was apparently the combined effect of many individual spots of porosity.

Figure No. 29 is a photograph of the X-ray film taken of the outer shroud weld in the second dummy welded and brazed showing the fewer iso-lated areas of porosity that existed. This improvement in the porosity condition as noted in Figure No. 28 has been attributed to the carbide burr polishing of the blade to remove all effects of glass bead blast.

The radiographic inspection of the outer shroud revealed, in addition to the porosity condition, one area at the leading edge of the vane to outer shroud joint to be cracked through the electron-beam weld. This appeared to correlate with the findings of the gas leak check.

Figure No. 30 is a normal X-ray exposure through the hub section. All blades appear to be welded. The weld appears to be generally porosity-free except for one small area in the lower right hand side of the photo-graph. This area of less dense material is probably some separate spots of porosity across the airfoil section being superimposed in one area.

c. Zyglo Inspection

The Zyglo inspection performed on the dummy assembly after final machining did not reveal any surface indications. It was anticipated that the microfissuring at the nail head of the electron-beam weld would show on the

Figure 28
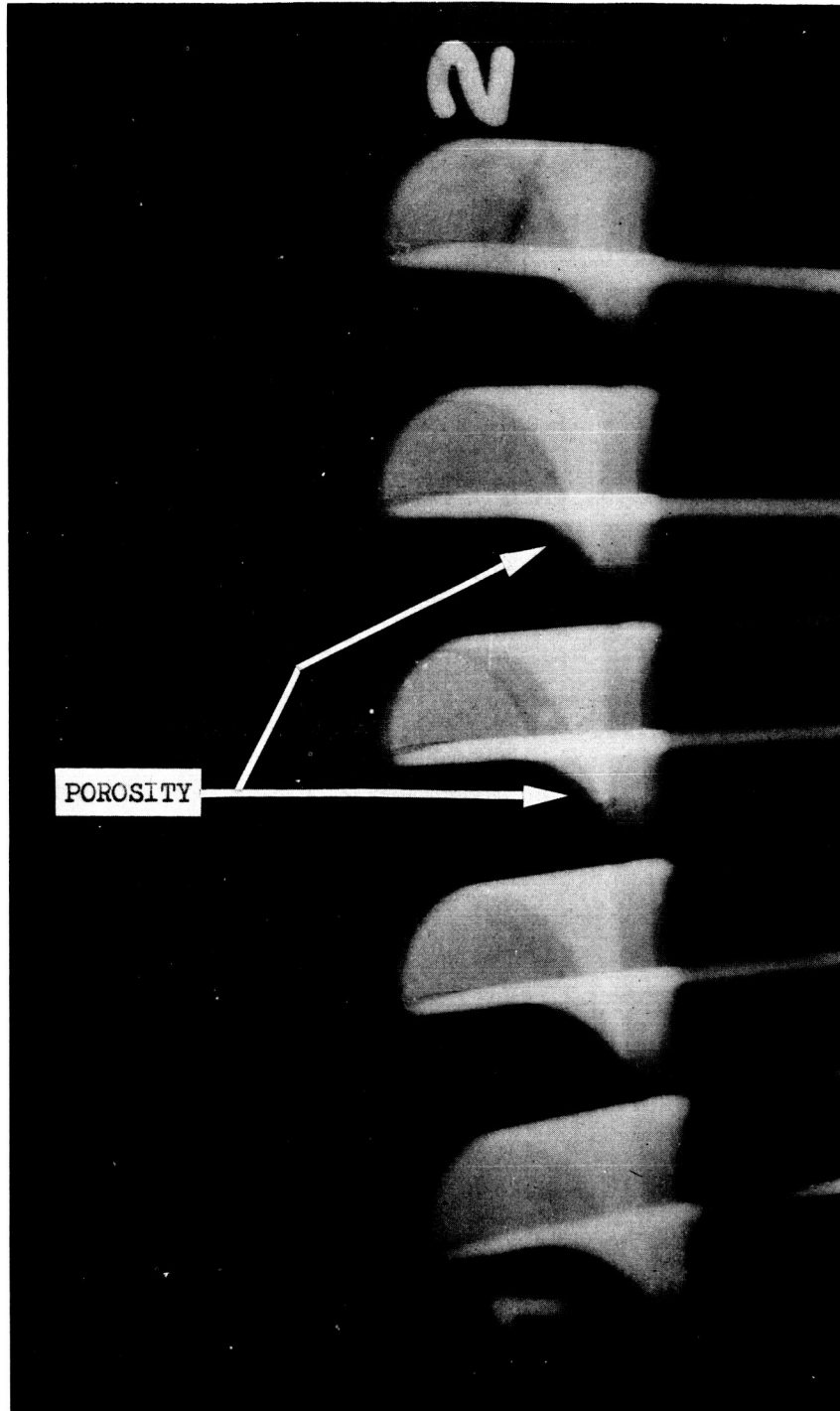
Photograph of the X-ray Film Showing the Porosity Condition
Which Existed in the Shroud-to-Blade Weld of the First
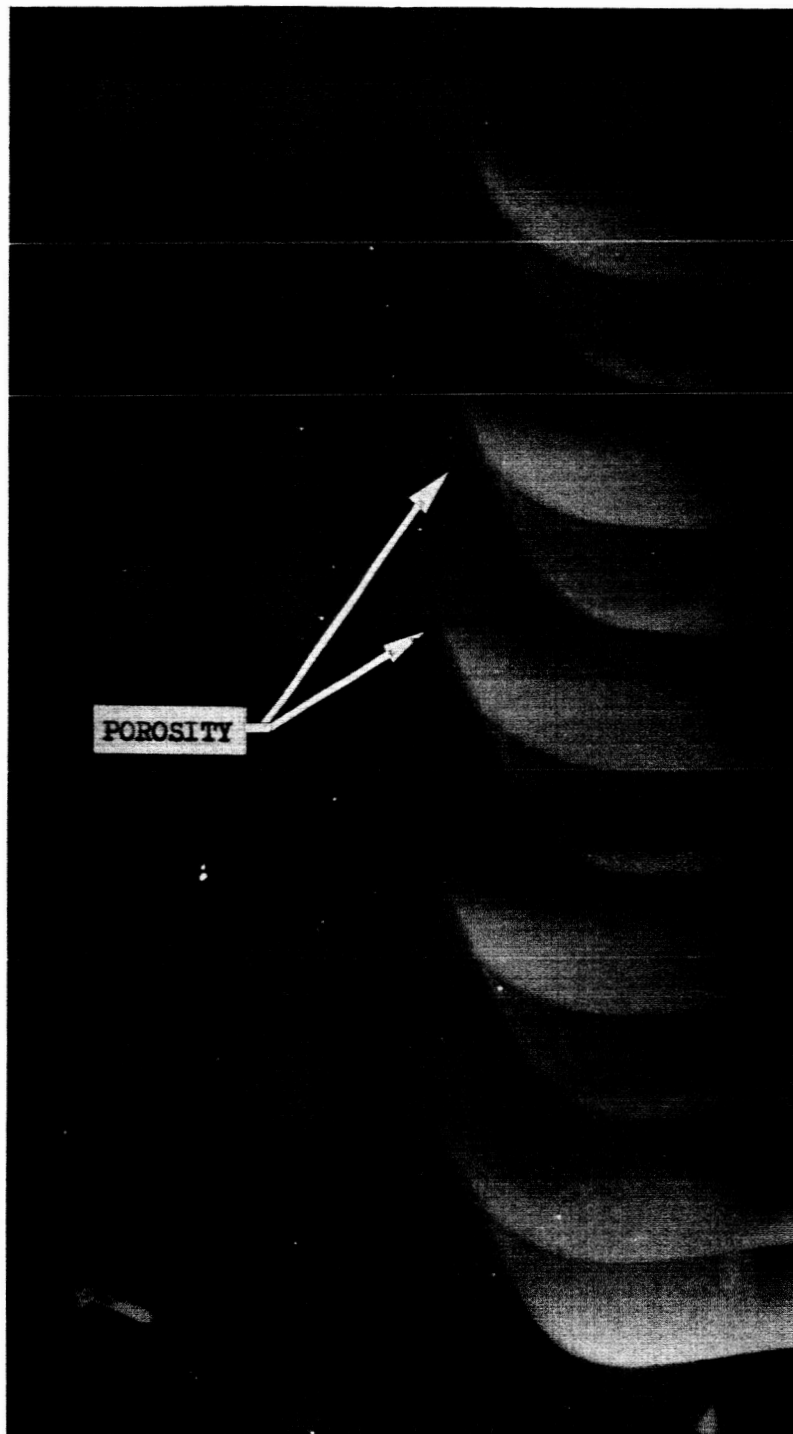Second-Stage Dummy

Figure 29

Photograph of the X-ray Film Showing the Porosity Condition
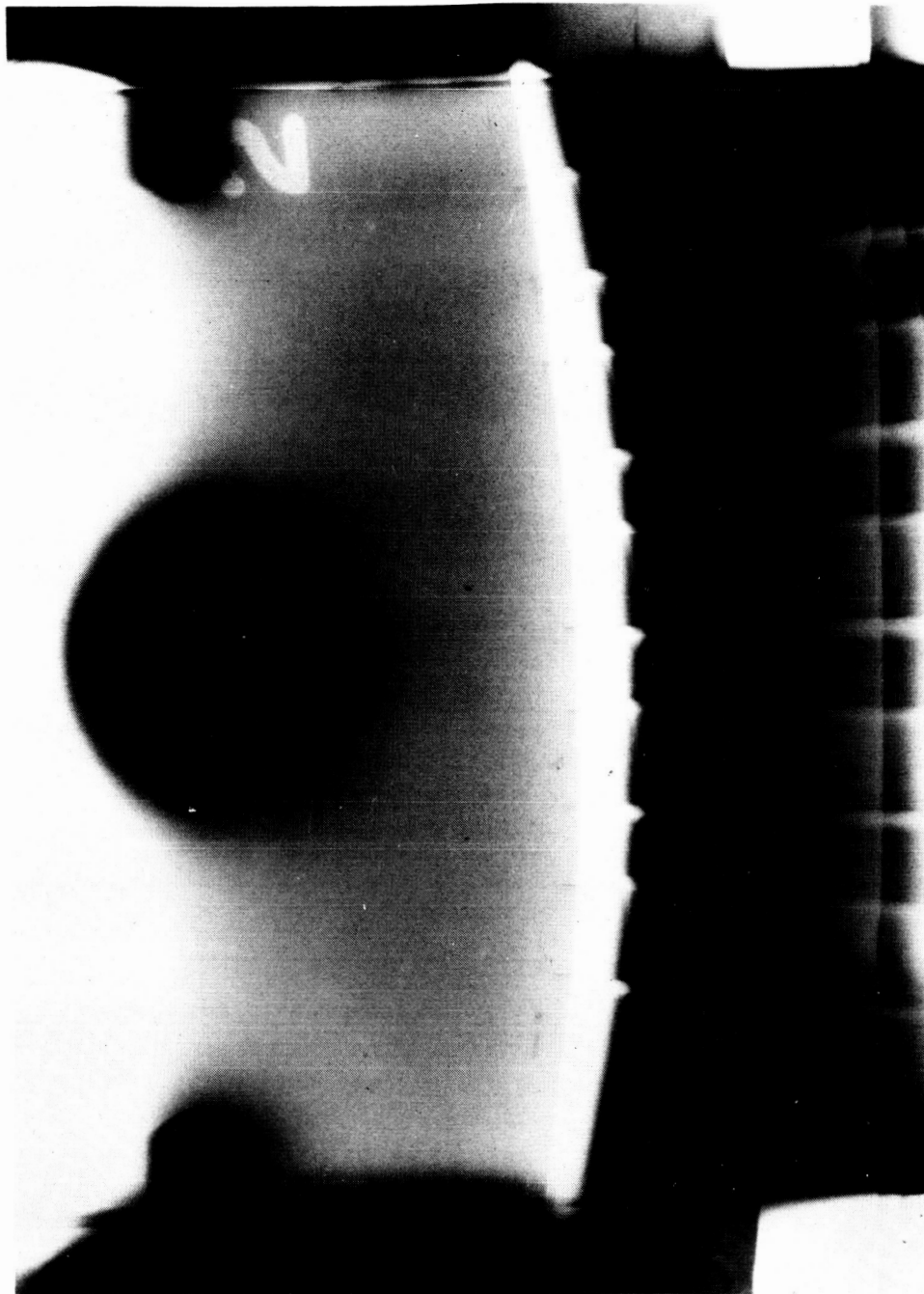Existing in the Shroud-to-Blade Weld of the Second-Stage Dummy

Page 43

Figure 30

Photograph of the X-ray Film Showing the Electron-Beam Weld
Area of the Blade-to-Center-Hub Joint

Page 44

final Zyglo. The fissures were most severe in this nail head area which was approximately 0.100-in. below the surface of the part. Because 0.100-in. was the clean-up removed during final machining, the surface examined by Zyglo should have contained the worst condition of fissuring in the part.

The reason for the microfissures not being revealed by Zyglo can be attributed to their being too small in length and/or too tight in width to retain the Zyglo oil. Possibly, a more stringent penetrant inspection operation, such as dye check or post-emulsion Zyglo would have revealed these fissures. Another possible reason for the microfissures not showing on Zyglo may be the result of the smearing tendency of this material during machining. This alloy machines very poorly and even in the aged condition, is quite gummy; thus, a great deal of smearing is observed.

d. Tensile Testing

The objective of testing the heat-treated blade segment shown in Figure No. 27 was to establish the mechanical strength of the weld joint, and thereby to obtain an estimate of the reduction in joint efficiency attributable to porosity and microfissuring.

Upon loading the vane assembly in tension, the shroud pulled from the blade at 15,000 lb corresponded to a shear stress of 67,000 psi. Two of the blades were retested with the load being applied through the shroud plugs. These shroud plugs pulled out of the vane at an average load of 10,400 lbs. After a load of 27,500 lb was applied to the blade segment tested by gripping the airfoil in flat jaws, the 1/2-in. threaded adaptor in the hub end broke.

The blade-to-shroud weld broke at a lower load than anticipated. With a minimum ultimate strength of 175,000 psi for this material, the breaking shear stress should have been approximately 100,000 psi. The reason for the premature failure of the shroud joint was found in the pull fixture which loaded the joint locally, failing one side of the joint prematurely. However, under much less than maximum operating conditions, the shear stress in the blade-to-shroud joint is 2700 psi, which is also much less than the tested value.

The blade-to-hub joint could not be tested to destruction because the holding fixture failed. At the time that the fixture failed, the average stress in the butt joint (blade-to-hub) was 112,000 psi as compared to a maximum combined local operating stress of 27,000 psi. It appeared that the joints, despite microfissuring and some porosity, were acceptable for this application.

An examination of the fractured surfaces of the tested blades showed the weld to be continuous around the blade and to contain a nominal amount of scattered porosity.

e.   Metallographic Inspection

The metallographic specimens taken through the electron-beam weld joining the blade to the hub revealed the two electron-beam welds to be continuous with each having approximately 1.100-in. penetration. This provided approximately 0.100-in. overlap (see Figure No. 31). The nail head of the weld measured 0.190-in. wide and 0.100-in. deep. The weld width ranged from 0.085-in. below the nail head to 0.050-in. in the center of the weld. Some porosity was noted in the cross-section; this had a maximum size of 0.020-in. Many very small pores were noted along the edges of the weld.

At the intersection of the blade to the hub, the weld was found to be sound with no signs of interface cracking propagating into the weld (see Figure No. 32).

Microfissures, approximately 0.020-in. long, were noted beneath the nail head of the electron-beam weld. These occurred in the parent metal immediately adjacent to the weld. Microfissures were also prevalant along the length of the entire weld; these had lengths of only 0.005-in. maximum and were separated generally by 0.030-in. to 0.050-in. Figure No. 33 is a typical photomicrograph taken of the electron-beam weld in the hub after brazing and aging. Microfissuring can again be observed along the edge of the weld. These were approximately of the same magnitude as was noted prior to brazing and aging.

The metallographic specimens made through the electron-beam weld in the outer shroud also showed the weld to be continuous. The results were nearly identical to the blade-to-hub weld with microfissuring found adjacent to the nail head. Also, micro-cracking along the length of the weld had the same length as those in the hub weld, but tended to be more frequent and more open in appearance. Porosity was found to be concentrated along the edge of the weld and tended to be more severe than in the hub weld.

Figure No. 34 is a photomicrograph made of the electron-beam weld in the outer shroud after brazing and aging. The microfissures did not appear to propagate during the heat treat cycle. Actually, the fissuring condition appeared less severe in these micros than in those made prior to heat treatment.

Figure No. 35 is a photograph of the blade-to-extension weld. Only one small fissure near the nail head of the electron beam weld, approximately 0.005-in. in length, could be detected. Other than this one fissure, the weld appeared to be sound and have good penetration as well as fusion characteristics.

The Nicro braze shown in Figure No. 36 appeared to be continuous around the blade; however, the fillet size, which according to the blueprint was to measure 0.020-in., measured 0.010-in. in some areas. Increasing the amount of braze alloy to produce a large fillet only resulted in increasing the braze buildup at the low point in the assembly. Apparently, the good fluidity of the molten braze alloy prevents obtaining a 0.020-in. minimum fillet size. From Figure No. 36, it can be seen that the braze penetrated the entire depth of the blade slot in the hub, or 0.450-in.
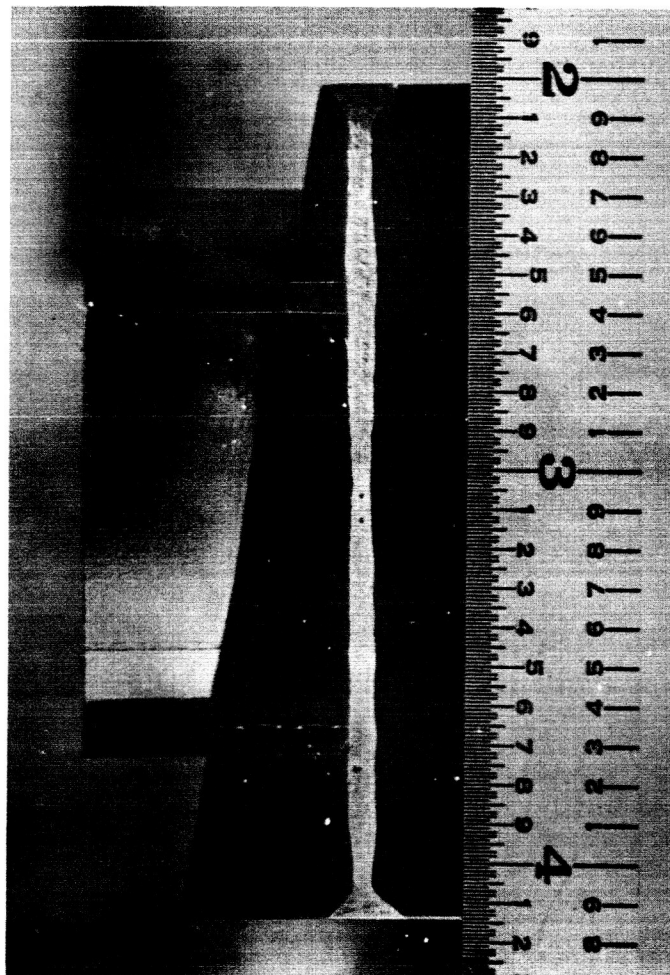
Figure 31

Photomicrograph of Electron-Beam Weld in the Hub Section of the Dummy Rotor

Mag: 50X

Figure 32

Photomicrograph of Electron-Beam Weld Joint at the Junction of the Blade and Hub
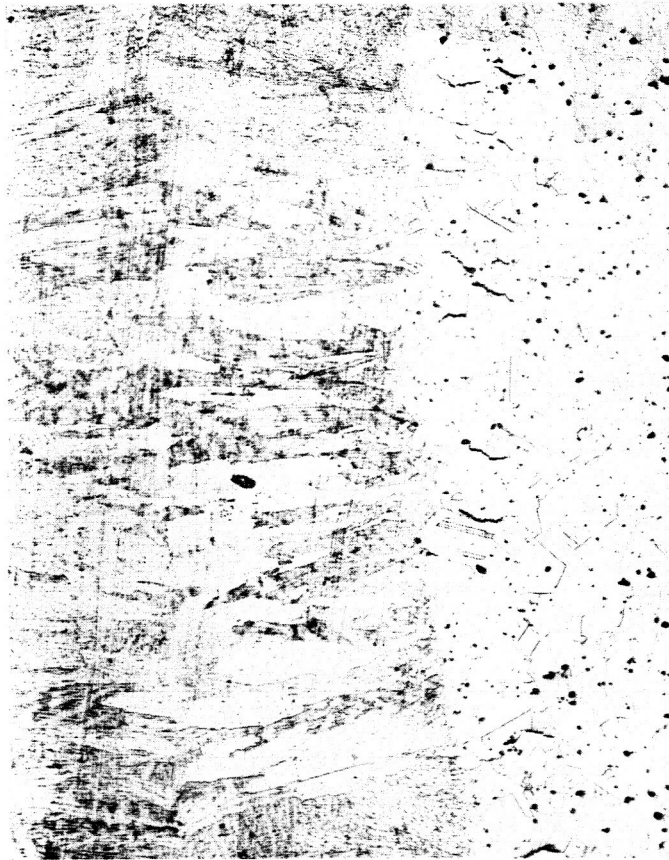
Mag: 50X

Figure 33

Photomicrograph of the Electron-Beam Weld in the Hub Section
of the Dummy Rotor Showing the Microfissuring Condition
Immediately Below the Nail Head
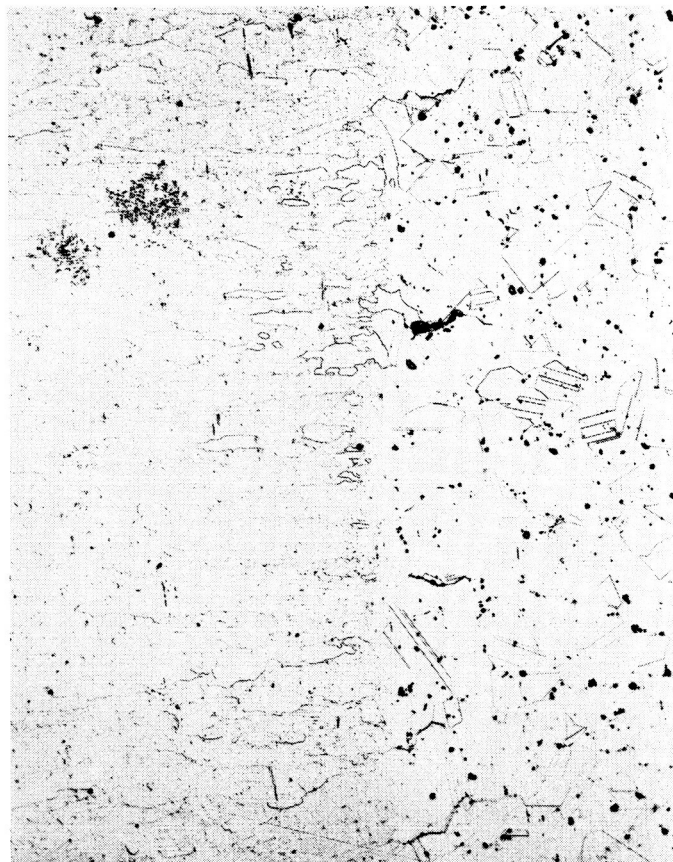
Mag: 50X

Figure 34

Photomicrograph of the Electron-Beam Weld in the Outer Shroud
Section After Brazing, Aging, and Finish Machining

Page 50
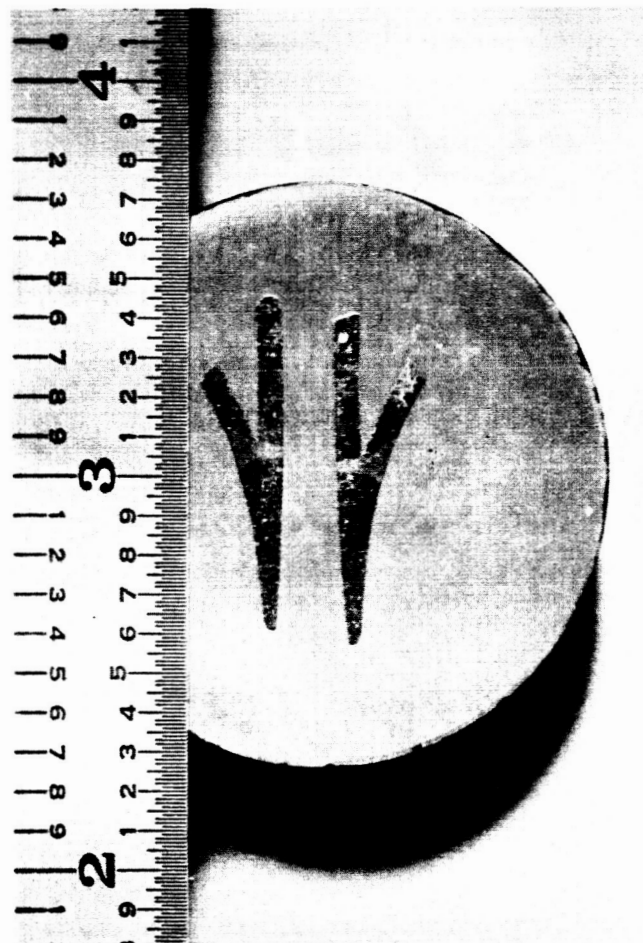
Figure 35

Photomacrograph of the Electron-Beam Weld Joining the Blade
to the Trailing Edge Extension

Page 51
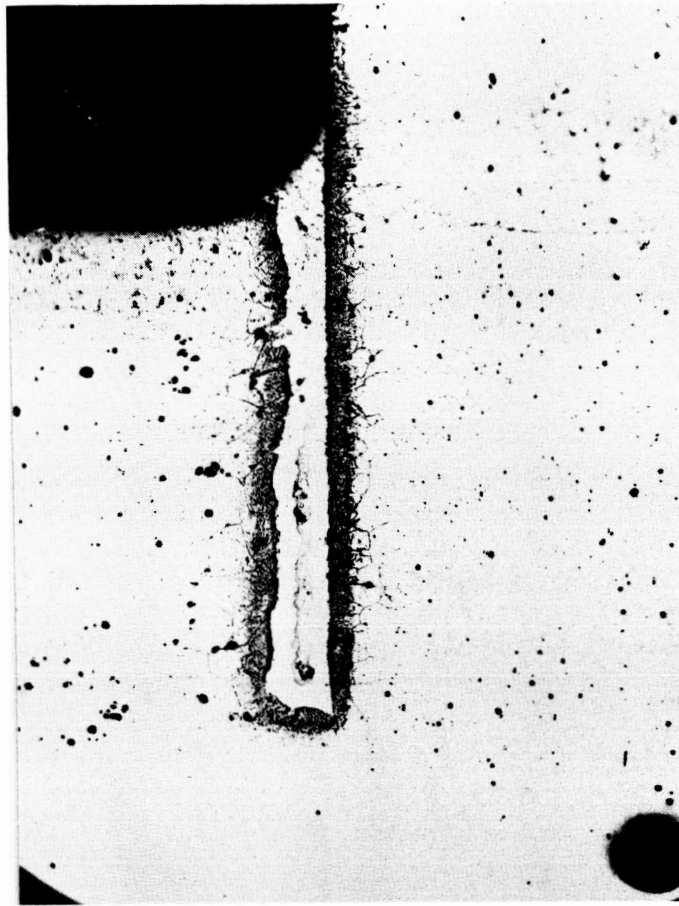
Mag: 50X

Figure 36

Photomicrograph Showing Nicro Braze Fillet Size and Penetration
in the Hub Section of the Second-Stage Dummy Assembly

Page 52

A metallographic evaluation of the electrical discharge machined surface did not show any affected surface layer. Initial metallographic studies made on some of the first vane slots produced by electrical discharge machining revealed surface irregularities approximately 0.002-in. deep. The coating or material in the affected zone caused problems during EB welding and it was found necessary to mechanically polish the surface to remove approximately 0.002-in. The maximum allowable gap width of 0.008-in. was maintained even with this material removed.

7. Conclusions

The fabrication of the dummy rotors fully confirmed the conclusions of the pre-dummy rotor weld development. It also proved that the EB weld joints could be made sufficiently strong for application to the M-1 oxidizer turbine rotors and stators. Optimum weld schedules were developed and tooling demonstrations were achieved.

F. FABRICATION OF ROTOR ASSEMBLIES

The dummy rotor program proved to be an excellent preparation for the manufacturing of the prototype rotors and stators. The techniques developed in the manufacturing of the dummies and the tooling experience was directly applied to the prototype hardware. The problems encountered in the fabrication of the prototype hardware were either identical or of a similar nature to those encountered fabricating the dummy rotors. Therefore, the discussion of the fabrication of the prototype hardware has been abbreviated to avoid redundancy.

Utilizing the machining, cleaning, and welding procedures established in the dummy rotor program, the first-stage and second-stage rotors were rough fabricated. Figure No. 37 shows the EB weld fixture used for welding the second-stage rotor. Copper chill-down blocks were used extensively as a heat sink to prevent erosion of the shrouds and to minimize distortion. The weld schedules utilized for the EB welding of the prototype blades sheet metal section to the trailing section, the EB welding the prototype blades to prototype discs and shrouds are shown in Figures No. 20 and No. 25, and Appendix A. These schedules were identical to those used for welding the dummy rotors.

X-ray inspection revealed a nominal amount of porosity.

Visual inspection of the first-stage rotor showed large gaps, up to 0.025-in., on a number of blades between the blade and the shroud, with a cracked joint. The large cracks were attributed to clearance accumulation of the shroud-to-blade, blade-to-plug, plug-to-blade, and blade-to-shroud clearances, resulting from weld shrinkage. To minimize the clearance accumulation in future assemblies, blades and plugs were plated with pure nickel to reduce the initial assembly clearance before welding. The drawing requirement for a maximum clearance of 0.008-in. proved to be excessive. Areas where the large gaps already existed were filled with pure nickel shim stock prior to brazing to assure a good braze joint.
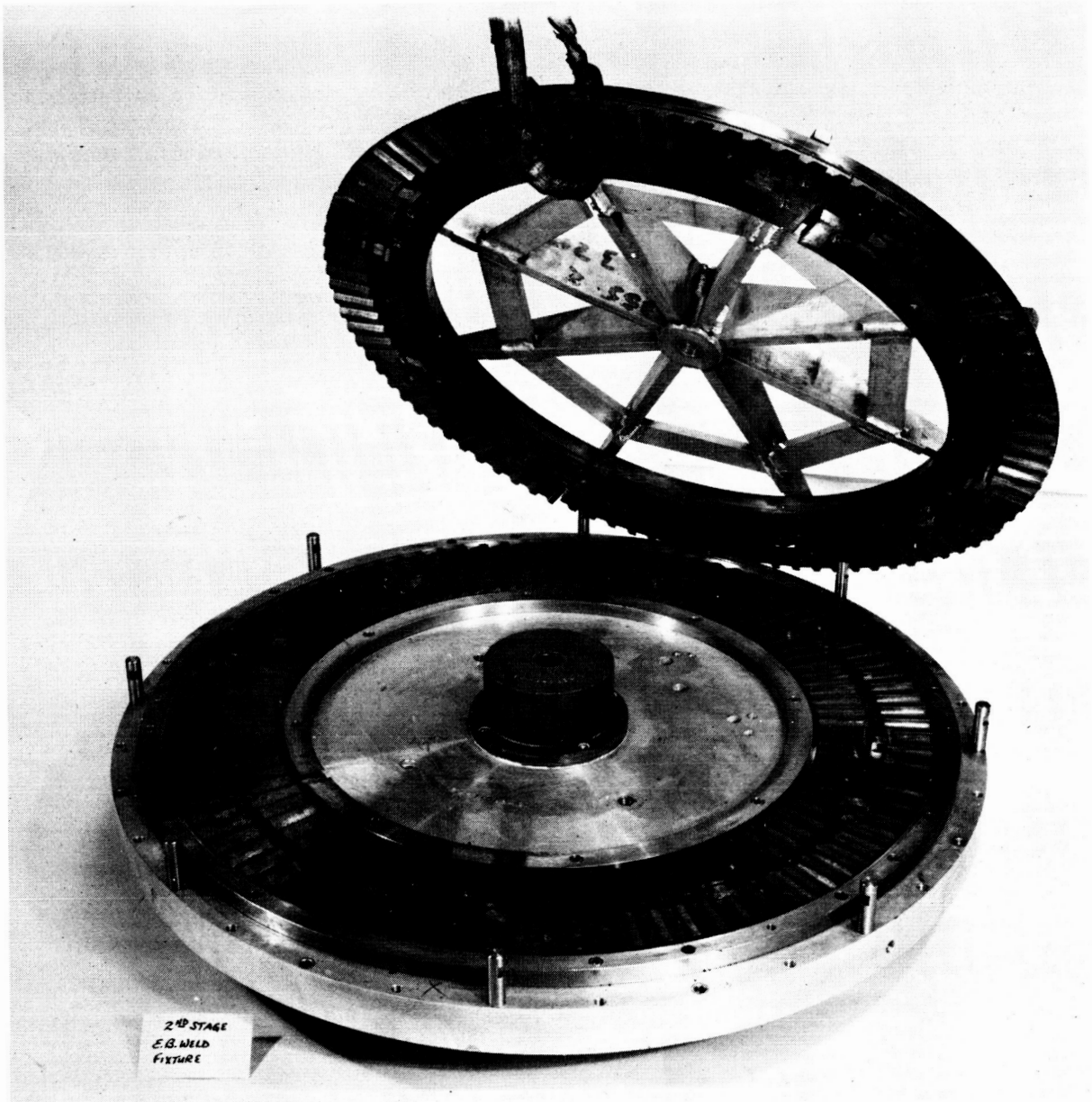
Figure 37

Electron-Beam Weld Fixture for Second-Stage Rotor

Page 54

Excess braze tended to accumulate at the trailing edge and close the trailing edge relief (see Figure No. 38). For this reason, it is better to braze such assemblies with the leading edge down.

Figures No. 38 and No. 39 show the major characteristics of the two rotors in the final machined condition.

G. FABRICATION OF STATOR ASSEMBLIES

The fabrication experience gained with the dummy rotors and with the prototype rotors was directly applicable to the fabrication of the stators with the exception of the EB welding of the nozzle. In the latter instance, considerable weld schedule development was necessary because of the required total penetration depth of 3.16-in., or 1.8-in. per beam. This weld development was conducted using nozzle samples containing three nozzle vanes (see Figure No. 40), which were welded in the prototype weld fixture shown in Figure No. 41. Despite the extensive use of copper chill-blocks, excessive melting occurred with weld schedules giving the full spike length of 1.8-in.

Figure No. 40 shows the effects of this excessive melting. Further weld development indicated that full penetration of the shroud with beams from both sides could be obtained without excessive melting provided high (55 KV) beam power was used and an Inconel 718 weld wire was placed into the vane slot as shown in Figure No. 42. This stop wire prevented the end of the vane from melting off and thus allowed for the second beam close to the end of the vane. Table I shows the successful weld schedules used to weld the prototype nozzle assembly.

Figures No. 43 and No. 44 show the major over-all dimensions in the final machined condition for the nozzle and vane stator assemblies.

X-ray inspection revealed porosity in the weld areas of both stators. Again, the braze was accumulated at the trailing of the stator vanes because of the hardware position during brazing. The availability of brazing furnaces necessitated that the stator assemblies be brazed in an argon atmosphere, rather than a vacuum; however, there was no noticeable effect upon the braze quality.

IV. CONCLUSIONS AND RECOMMENDATIONS

The process of electron-beam (EB) welding was used to fasten hollow sheet metal blades to rotor discs as well as to rotor and stator shrouds. The basic design philosophy, although an advanced technology, proved successful for the M-1 oxidizer turbine.

High initial tooling costs necessitate a recommendation that the design be used only for application with six or more units.

Further material and weld development of Inconel 718 is needed to reduce microfissuring and porosity if this design concept is to be used for very high stress components.
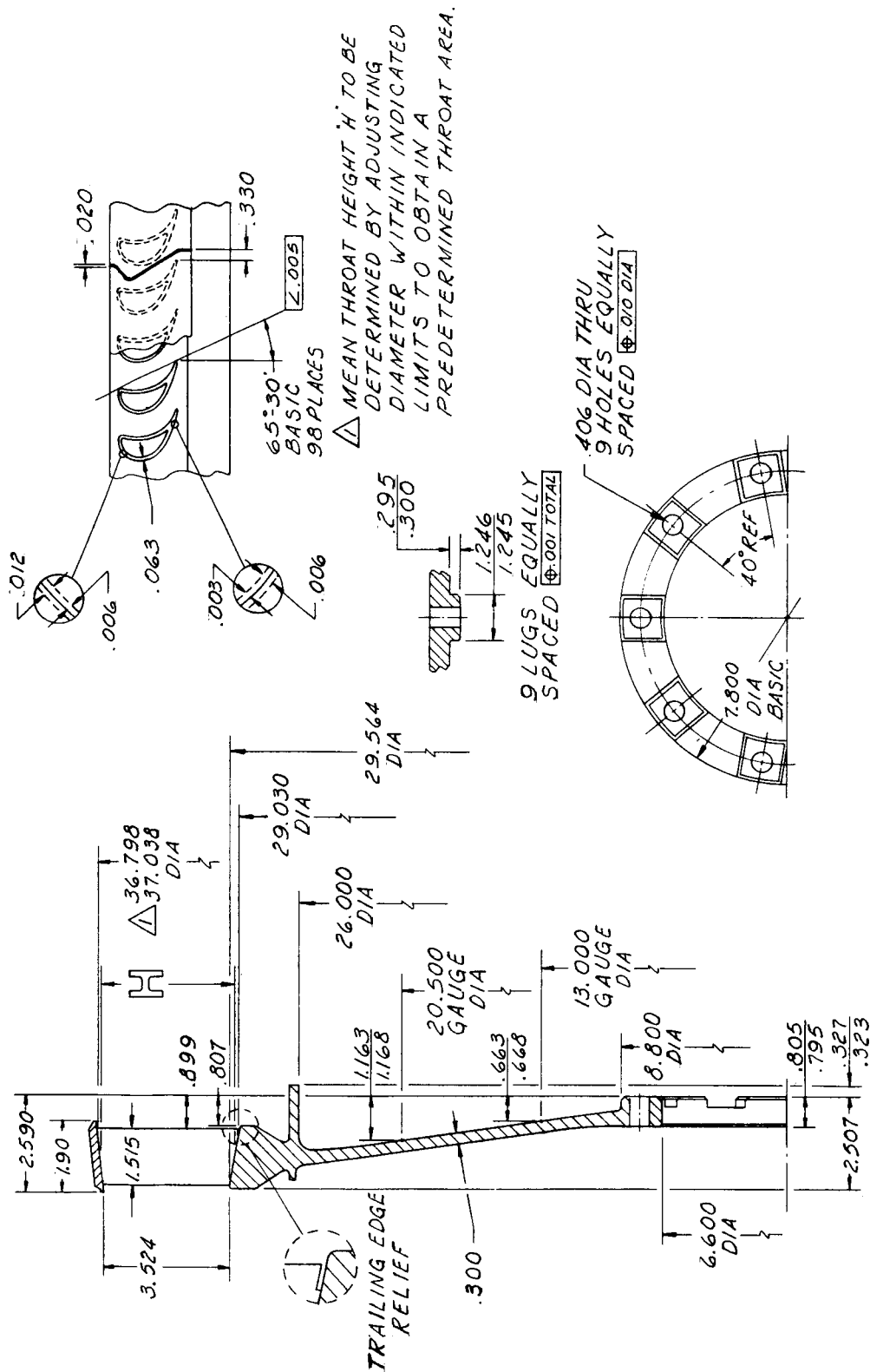
Figure 38

Rotor Assembly - Stage 1

Page 56

Figure 39

Rotor Assembly - Stage 2

Page 57
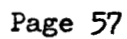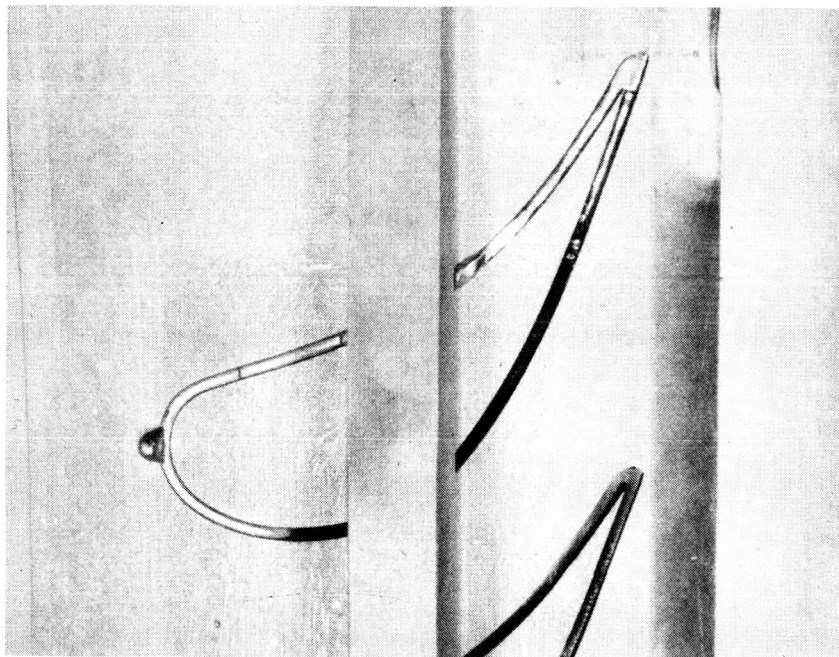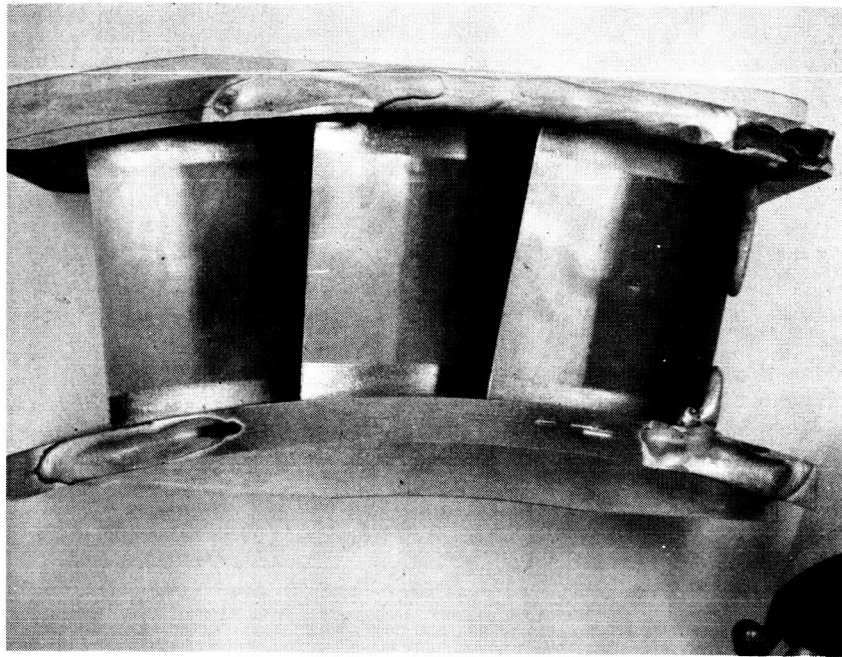
Figure 40

Excessive Melting on Nozzle Weld Samples
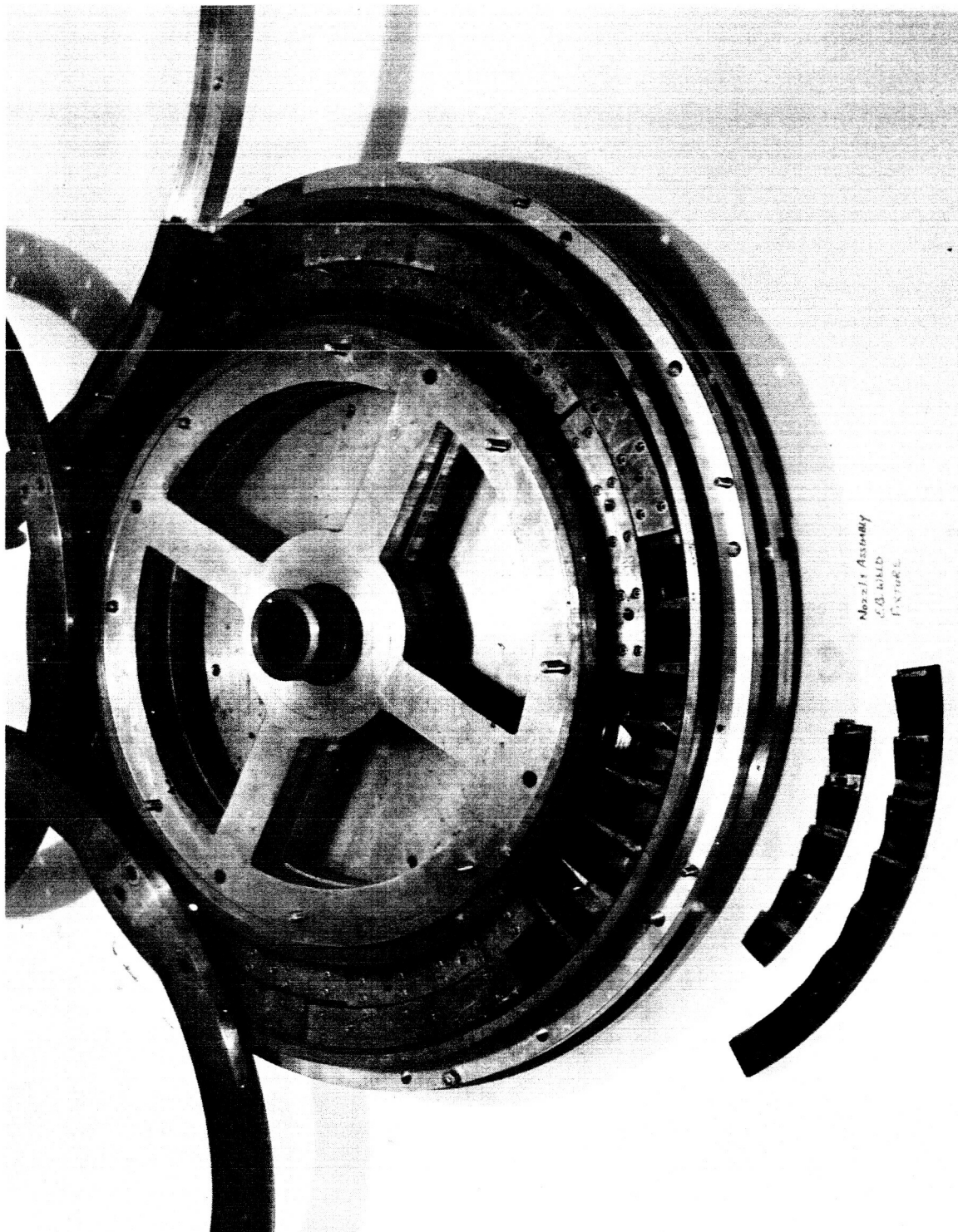
Figure 41

Electron-Beam Weld Fixture for Nozzle

BUTT JOINT
ONE SPIKE

3.600

OUTER
SHROUD

.52

.180

36.200
DIA

SHEAR JOINT
TWO SPIKES

.180

INNER
SHROUD

.52

.060

.06

MELTED
MATERIAL

PREPLACED
INCO 718 WELD
WIRE

29.800
DIA
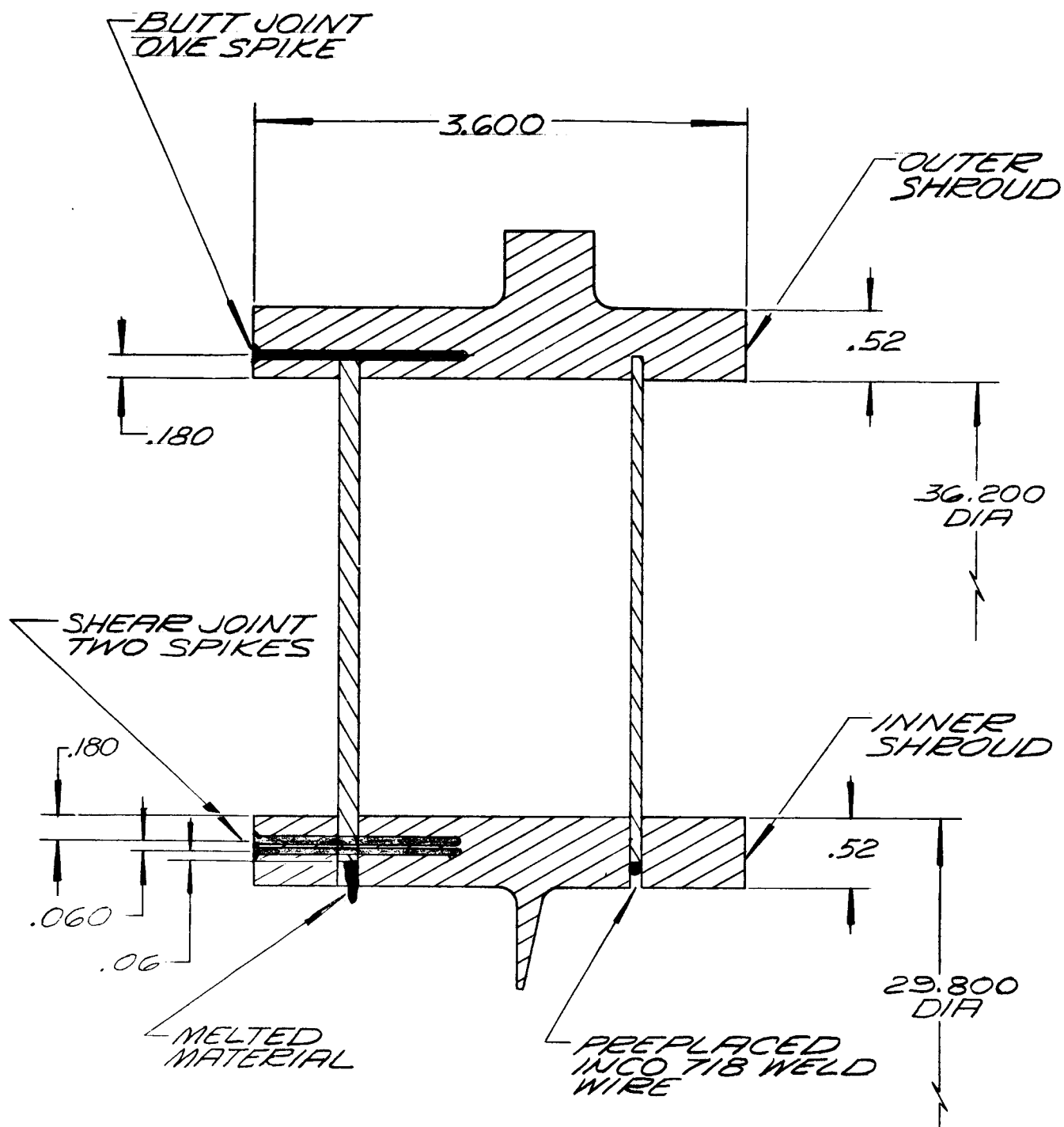
Figure 42

Nozzle Electron-Beam Weld Spike Positions

Page 60

TABLE I

WELD SCHEDULE FOR NOZZLE ASSEMBLY

High Voltage - 55 KV

Slope Rate - 3

Milliamperes - 320

Focus Pot "Ref" 308 "AMPS" 5.6

Filament Current - 58

Movement of Part (IPM) - 35

Direction - Right

Gun to Work Distance - 3.500 Inches

Filament Size - 500 MA

Filament to Cathode Distance - .381 Inches

Spacer - 350 MA

Anode Type - 60 KV

Cathode Type - 500 MA

Angle of Gun to Work Piece - 90°

Power Supply Frequency - 60 Cycle 440V

.006 MAX

.006 MAX

.003 MAX

.003 MAX

49°30' BASIC
13 PLACES

∠.005

TRAILING EDGE
RELIEF

⚠ MEAN THROAT HEIGHT "H" TO BE
DETERMINED BY ADJUSTING
DIAMETER WITHIN INDICATED
LIMITS TO OBTAIN A PREDETERMINED
THROAT AREA.

36.200
DIA

H

⚠ 29.900
29.700
DIA

1.515

.100

3.350

.410

37.060
DIA

2.740

.200

2.195

38.100
DIA

79.060
DIA
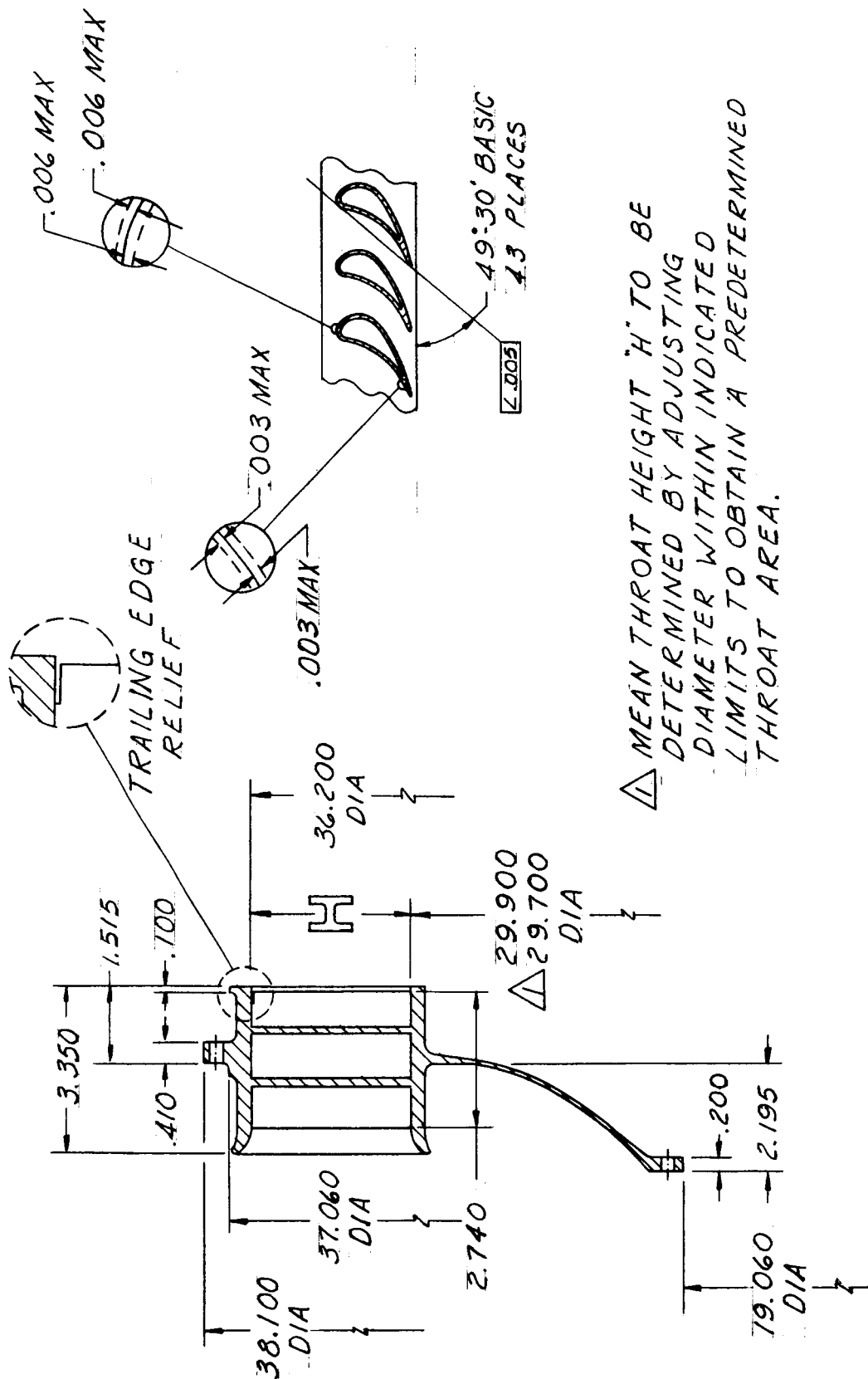
Figure 43

Nozzle Assembly

Figure 44

Reversing Vane Assembly

Page 63
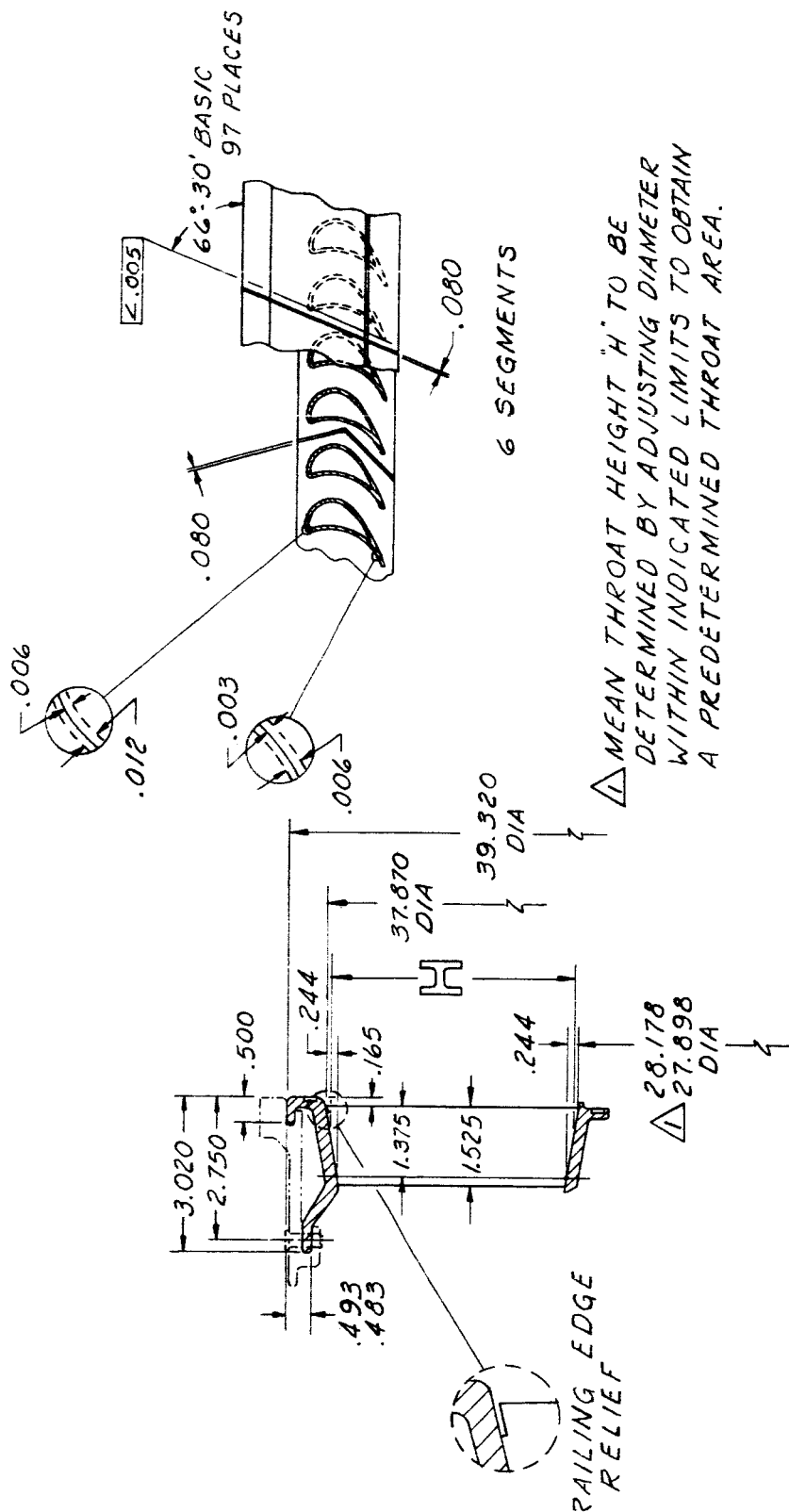
Extremely close tolerance and system matching of the blade and the slot are costly manufacturing methods. In future designs, other methods of attachment should be evaluated to produce a design that would eliminate any need for close tolerances and system matching without imposing excessive tooling costs.

BIBLIOGRAPHY

1. Beer, R., <u>Aerodynamic Design and Estimated Performance of a Two-Stage Curtis Turbine for the Liquid Oxygen Turbopump of the M-1 Engine</u>, NASA Report No. CR 54764, 19 November 1965

2. Inouye, F. T., Hunt, V., Janser, G. R., and Frick, V., <u>Summary of Experience Using Alloy 718 for M-1 Engine Components</u>, NASA Report No. CR 54814, 15 July 1966

3. Kane, R. F., <u>Aerojet-General M-1 Oxidizer Program, Evaluation of Second-Stage Dummy Rotor, S/N 1</u>, Thompson-Ramo-Wooldridge, Inc., May 1965

4. Roesch, E., <u>Mechanical Design of a Curtis Turbine for the Oxidizer Turbopump of the M-1 Engine</u>, NASA Report No. CR 54815, 15 June 1966

APPENDICES

APPENDIX A

FURNACE BRAZING PROCEDURE

FURNACE BRAZING PROCEDURE

TRW INC.
23555 Euclid Avenue
Cleveland 17, Ohio

1. **Scope:** To establish the brazing procedure for the listed Inconel 718 assemblies.

2. **Customer:** Aerojet General Corporation, Sacramento, California

3. **Purchase Order No.:** 150025

4. **Applicable Assemblies:**

F.R.	C.P.N.	Description
401200	286528-1	1st Stg. Turbine Disc
401225	286529-9	Dummy Rotor
401250	286533-1	2nd Stg. Turbine Disc
401275	286532-9	Dummy Rotor
401300	286545-9	Oxidizer Turbine Stator Vane
401317	286513-19B	Turbine Nozzle Assembly

5. **Blueprint Requirements:** After welding, braze blades per applicable portion of AMS 2675 in vacuum furnace at 1 to 5 microns. Hold at 1900 to 1950°F for 10 minutes, then cooled at room temperature.

6. **Materials:**

   6.1 Type of base material being brazed:
   AGC 44151 (Inconel 718)
   AGC 44152 (Inconel 718)

   6.2 Type of brazing alloy: AMS 4777 (LMW)
   Nicrobraze (LMW) is braze alloy per AMS 4777 modified by addition of proprietary flux.

   6.3 Binder: Meta chem 4

7. **Equipment:** Assemblies shall be brazed in an Ipsen Vacuum Furnace VFC 48 x 48 x 36 (24) located at TRW, 23555 Euclid Ave., Cleveland 17, Ohio

8. **Procedure for brazing:**

   8.1 Assembly shall be wiped clean with acetone.

   8.2 Apply braze material in a 0.090" fillet completely around the airfoil at the interface of the vane to the outer shroud and at the interface of the vane to the inner shroud or disc.

   8.3 Assembly part on support type fixturing.

   8.4 Place assembly into furnace.

8.5 Attach two monitor thermocouples to thickest and thinnest cross sections of assembly. Attach a third thermocouple to fixture.

8.6 Attach 6 Inconel 718 sheet stock (AGC 44152) tensile specimens to assembly.

8.7 Pump down to 1 micron or less prior to application of heat.

8.8 Equalize at 1000°F ± 25 and then again at 1740°F ± 10. If pressure exceeds 5 microns, the heat shall be turned off to allow the furnace vacuum to recove to 2 microns. Equalizing temperature shall be maintained for fifteen minute: or until the pressure reading is less than 2 microns, which ever is longer.

8.9 Raise temperature to 1925°F ± 25 as rapidly as possible and hold within this temperature range for 10 minutes.

8.10 Back fill with argon (99.995 purity) and cool to 1750°F.

8.11 Turn fan on when temperature reaches 1750°F and cool to below 150°F.

9. Braze requirements: 0.020" to 0.060" braze fillets at blade to disc and blade to shroud points.

10. Inspection: Braze quality shall be visually inspected for conformance to Paragraph 9.

11. Rework: Areas with lack of braze in excess of the limits specified shall be re-brazed in accordance with Section 8.

12. Records: The Strip Chart shall be a record of the temperature indicated by the thermocouples specified in Paragraph 8.5 and the following information shall be recorded on the Strip Chart.

    1. Date of treatment.
    2. Specification to which part was brazed.
    3. Furnace type and identity.
    4. Part number and serial number.
    5. Time scale of Strip Chart.

R. F. Kane
Metallurgical Engineer
Materials Engineering Department

RFK/cmc

APPENDIX B

HEAT TREAT PROCEDURE

HEAT TREAT PROCEDURE

TRW INC.
23555 Euclid Avenue
Cleveland 17, Ohio

1. Scope: To establish an Aging Procedure for listed Inconel 718 Assemblies.

2. Customer: Aerojet General Corporation, Sacramento, California.

3. Purchase Order No.: 150025

4. Applicable Assemblies:

F.R.	C.P.N.	Description
401200	286528-1	1st Stg. Turbine Disc
401225	286529-9	Dummy Rotor
401250	286533-1	2nd Stg. Turbine Disc
401275	286532-9	Dummy Rotor
401300	286545-9	Oxidizer Turbine Stator Vane
401317	286513-19B	Turbine Nozzle Assembly

5. Blueprint Requirements: After brazing, age per AGC-46604.

6. Base Material: AGC-44151 Inconel 718
AGC-44152 Inconel 718

7. Equipment: Ipsen Vacuum Furnace - VFC 48 x 48 x 36 (24)
Located at - TRW, 23555 Euclid Ave., Cleveland 17, Ohio

8. Procedure for Aging.

   8.1 Wash with acetone.

   8.2 Assemble on support type fixturing.

   8.3 Attach two monitor thermocouples to thickest and thinnest cross sections of assembly; attach a third thermocouple to fixturing.

   8.4 Attach 6 Inconel 718 Sheet Stock (AGC-44152) tensile specimens to assembly.

   8.5 Pump down to 1 micron or less prior to application of heat.

   8.6 Equalize at 1000°F ± 25. If pressure exceeds 100 microns the heat shall be turned off to allow the furnace vacuum to recover to below 10 microns. Equalizing temperature shall be maintained for fifteen minutes or until the pressure reading is less than 10 microns which ever is longer.

   8.7 Raise temperature to 1350°F, ± 15, hold at 1350°F for 8 to 10 hours, furnace cool to 1200°F, hold at 1200°F until a total aging time of 20 hours has elapsed (1350°F + furnace cool + 1200°F).

8.8 Back fill with argon (99.995 Purity), and fan cool to 150°F before discharging from furnace.
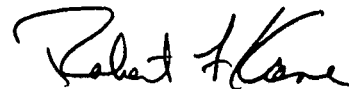
9. Inspection:

9.1 Check and record hardness of test samples and assembly; Rc 38 min. required.

9.2 Send test samples to Materials Engineering Laboratory for testing to requirements of AGC STD 4861 paragraph 3.2.1.

10. Records: The Strip Chart shall be a record of the temperature indicated by the thermocouples specified in paragraph 8.4 and the following information shall be recorded on the Strip Chart.

1. Date of treatment.
2. Specification to which part was heat treated.
3. Furnace type and identity.
4. Part number and serial number.
5. Time scale of Strip Chart.
6. Hardness of part and test samples.

R. F. Kane
Metallurgical Engineering
Materials Engineering Dept.

RFK/cmc

W. A. Tomazic (3 Copies)
NASA
Lewis Research Center
21000 Brookpark Road
Cleveland, Ohio 44135
Mail Stop 500-305

H. Hinckley (1 Copy)
Mail Stop 500-210

Patent Counsel (1 Copy)
Mail Stop 501-2

Lewis Library (2 Copies)
Mail Stop 60-3

N. J. Hartmann (1 Copy)
Mail Stop 5-9

W. L. Stewart (1 Copy)
Mail Stop 5-9

J. C. Montgomery (1 Copy)
Mail Stop 501-1 SNPO-C

Major L. Karalis (1 Copy)
AFSC Liaison Office
Mail Stop 4-1

Office of Reliability and
  Quality Assurance (1 Copy)
Mail Stop 500-203

W. F. Dankhoff (1 Copy)
Mail Stop 3-13

F. J. Dutee (1 Copy)
Mail Stop 23-1

D. F. Lange (1 Copy)
Mail Stop 501-1

J. B. Esgar (1 Copy)
Mail Stop 49-1

D. D. Scheer (1 Copy)
Mail Stop 500-305

C. F. Zalabak (1 Copy)
Mail Stop 500-305

NASA Representative (6 Copies)
NASA Scientific and Technical
  Information Facility
Box 5700
Bethesda, Maryland

Library (1 Copy)
NASA
George C. Marshall Space Flight Center
Huntsville, Alabama 35812

Library (1 Copy)
NASA
Western Support Office
150 Pico Boulevard
Santa Monica, California 90406

Library (1 Copy)
Jet Propulsion Laboratory
4800 Oak Grove Drive
Pasadena, California 91103

A. O. Tischler (2 Copies)
Code RP - NASA Headquarters
Washington, D. C. 20546

W. W. Wilcox (1 Copy)
Code RP - NASA Headquarters
Washington, D. C. 20546

J. W. Thomas, Jr. (5 Copies)
I-E-E
NASA
George C. Marshall Space Flight Center
Huntsville, Alabama

E. W. Gomersall (1 Copy)
NASA
Mission Analysis Division
Office of Advanced Research and Technology
Moffett Field, California 94035

Dr. Keith Boyer (1 Copy)
Los Alamos Scientific Laboratory
CMF-9
P. O. Box 1663
Los Alamos, New Mexico

A. Schmidt (1 Copy)
National Bureau of Standards
Cryogenic Division
Boulder, Colorado

Library (1 Copy)
NASA
Ames Research Center
Moffett Field, California 94035

Library (1 Copy)
NASA
Flight Research Center
P. O. Box 273
Edwards AFB, California 93523

Library (1 Copy)
NASA
Goddard Space Flight Center
Greenbelt, Maryland 20771

Library (1 Copy)
NASA
Langley Research Center
Langley Station
Hampton, Virginia 23365

Library (1 Copy)
NASA
Manned Spacecraft Center
Houston, Texas 77058

Chemical Propulsion Information
  Agency (1 Copy)
Johns Hopkins University
Applied Physics Laboratory
8621 Georgia Avenue
Silver Spring, Maryland

Robert O. Bullock (1 Copy)
Garrett Corporation
Airesearch Manufacturing Company
402 S. 36th Street
Phoenix, Arizona 85034

Library Dept. 586-306 (1 Copy)
Rocketdyne
Division of North American Aviation
6633 Canoga Avenue
Canoga Park, California 91304

John Stanitz (1 Copy)
Thompson-Ramo-Wooldridge, Inc.
23555 Euclid Avenue
Cleveland, Ohio 44117

Dr. G. Wislicenus (1 Copy)
Penn State University
Naval Ordnance Laboratory
University Park, Pennsylvania

Dr. A. Acosta (1 Copy)
California Institute of Technology
1201 East California Street
Pasadena, California

Dr. E. B. Konecci (1 Copy)
NASA
Executive Office of the President
Executive Office Building
Washington, D. C.

Dr. M. Vavra (1 Copy)
Naval Post-Graduate School
Monterey, California

H. V. Main (1 Copy)
Air Force Rocket Propulsion Laboratory
Edwards Air Force Base
Edwards, California

Dr. George Serovy (1 Copy)
Iowa State University
Ames, Iowa

T. Iura (1 Copy)
Aerospace Corporation
2400 East El Segundo Blvd.
P. O. Box 95085
Los Angeles, California 90045

Pratt & Whitney Aircraft
  Corporation (1 Copy)
Florida Research and Development
  Center
P. O. Box 2691
West Palm Beach , Florida 33402

Dr. M. J. Zucrow (1 Copy)
Purdue University
Lafayette, Indiana 47907